Research in Astronomy and Astrophysics, 24:045018 (22pp), 2024 April https://doi.org/10.1088/1674-4527/ad30b2

BSN: Photometric Light Curve Analysis of Two Contact Binary Systems LS Del and V997 Cyg

Atila Poro[1], Mehmet Tanriver[2,3], Elham Sarvari[4], Shayan Zavvarei[5], Hossein Azarara[6], Laurent Corp[7], Sabrina Baudart[7], Asma Ababafi[8], Nazanin Kahali Poor[4], Fariba Zare[9], Ahmet Bulut[10,11], and Ahmet Keskin[2]

[1] Astronomy Department of the Raderon AI Lab., Burnaby, BC., Canada; poroatila@gmail.com
[2] Department of Astronomy and Space Science, Faculty of Science, Erciyes University, Kayseri TR-38039, Türkiye
[3] Erciyes University, Astronomy and Space Science Observatory Application and Research Center, Kayseri TR-38039, Türkiye
[4] Independent Astrophysics Researcher, Tehran, Iran
[5] Department of Physics, Shahid Beheshti University, Tehran, Iran
[6] Faculty of Physics, Shahid Bahonar University of Kerman, P.O.Box 76175, Kerman, Iran
[7] Double Stars Committee, Société Astronomique de France, Paris, France
[8] Dez Astronomical Association, Khouzestan Province, Dezful, Iran
[9] Department of Physics, Amirkabir University of Technology, Tehran, Iran
[10] Department of Physics, Faculty of Sciences, Çanakkale Onsekiz Mart University, Terzioğlu Kampüsü, TR-17020, Çanakkale, Türkiye
[11] Astrophysics Research Center and Observatory, Çanakkale Onsekiz Mart University, Terzioğlu Kampüsü, TR-17020, Çanakkale, Türkiye

Received 2024 January 17; revised 2024 February 19; accepted 2024 March 5; published 2024 April 17

Abstract

The light curve analyses and orbital period variations for two contact binary stars, LS Del and V997 Cyg, are presented in this work which was conducted in the frame of the Binary Systems of South and North project. Ground-based photometric observations were performed at two observatories in France. We used the Transiting Exoplanet Survey Satellite (TESS) data for extracting times of minima and light curve analysis of the target systems. The $O-C$ diagram for both systems displays a parabolic trend. LS Del and V997 Cyg's orbital periods are increasing at rates of $dP/dt = 7.20 \times 10^{-08}$ days yr^{-1} and $dP/dt = 2.54 \times 10^{-08}$ days yr^{-1}, respectively. Therefore, it can be concluded that mass is being transferred from the less massive star to the more massive component with a rate of $dM/dt = -1.96 \times 10^{-7} M_{\odot}$ yr^{-1} for the LS Del system, and $dM/dt = -3.83 \times 10^{-7} M_{\odot}$ yr^{-1} for V997 Cyg. The parameters of a third possible object in the system are also considered. The PHysics Of Eclipsing BinariEs Python code was used to analyze the light curves. The light curve solutions needed a cold starspot due to the asymmetry in the LS Del system's light curve maxima. The mass ratio, fill-out factor, and star temperature all indicate that both systems are contact binary types in this investigation. Two methods were applied to estimate the absolute parameters of the systems: one method relied on the parallax of Gaia DR3, and the other used a $P-M$ relationship. The positions of the systems are also depicted on the $M-L$, $M-R$, $q-L_{\rm ratio}$, and $\log M_{\rm tot} - logJ_0$ diagrams. We recommend that further observations and investigations be done on the existence of a fourth body in this system.

Key words: (stars:) binaries: eclipsing – methods: observational – stars: individual (LS Del and V997 Cyg)

1. Introduction

W Ursae Majoris (W UMa) type systems are categorized as eclipsing variables, with both components filling their Roche lobes, as described by Paczyński (1971). A common convective envelope is shared between the two components (Lucy 1968), in which mass and energy transfer from one component to the other. Consequently, despite having different features, the two components of contact binaries maintain nearly identical temperatures.

The orbital period of contact systems is typically $P_{\rm orb} \leqslant 1$ day, with most systems having a period of ∼0.2–0.6 days (Pribulla et al. 2003; Dryomova & Svechnikov 2006; Latković et al. 2021). Also, various studies have shown that some of the absolute parameters of stars in contact systems can have a significant relationship with the orbital period (Qian 2003; Gazeas & Stępień 2008; Kouzuma 2018). Additionally, it is known that contact binaries show significant magnetic activity, which affects orbital period fluctuations (O'Connell 1951; Applegate 1992).

Despite extensive studies conducted on W UMa-type systems, however, there are still many open questions regarding the physical and geometric features of the components and the formation and evolution of the system (Zhou et al. 2016).

We investigated two binary star systems. The first target in this study is LS Delphini (GSC 01656-01961). It was discovered by Bond (1976), who used the y filter in photoelectric observations. Observations showed that LS Del has a magnitude ranging from 8.66 to 9.17 in the V filter and an orbital period of 0.363842 days reported in the VSX database. Studies have been conducted regarding the light curve analysis of LS Del such as Maceroni & van't Veer (1996), Lu & Rucinski (1999), and Deb & Singh (2011). In all of the studies, the inclination was estimated to be less than 50°. Also, a noteworthy point in the analysis of the photometric light curve and with spectroscopic data is that this system's mass ratio is reported to be between 0.37 and 0.57.

The second system, V997 Cyg (GSC 03935-02233), is in the constellation Cygnus and was discovered by Cuno Hoffmeister (Hoffmeister 1963). It has a short orbital period of less than half a day (0.4582264[12] days), and its magnitude range in the V filter is between 13.16 and 13.61.[13] Initially, V997 Cyg was categorized as an RR Lyr type in the Sonneberg Obs. catalog (Gessner 1966), and it was later recognized as an eclipsing binary by the Akerlof et al. (2000) study. There were observations related to the V997 Cyg system, such as those in Devor et al. (2008).

This work is a continuation of the Binary Systems of South and North (BSN)[14] project's observations and analyses of eclipsing binary systems. Therefore, we employed ground-based observations and Transiting Exoplanet Survey Satellite (TESS) data for studying the binary systems LS Del and V997 Cyg. We present an analysis of the orbital period variations and a new ephemeris for each target system. Light curve solutions for both target systems are provided; moreover, the analysis of the V997 Cyg system is done for the first time. Additionally, two methods utilized used to estimate the systems' absolute parameters.

2. Observation and Data Reduction

The LS Del and V997 Cyg binary systems were observed in two observatories in France. The V standard filter was employed for observations at both observatories.

LS Del was observed on five nights during the summers of 2016, 2019, 2021, and 2023 at a private observatory (long 02 29 09 E, lat 44 15 38 N, alt of 661 m). We employed a 135mm Telelens and a Moravian G2 CCD for these observations. We had a total of 956 images with 60 seconds of exposure time. The average temperature of the CCD was −25 °C during the observations. Basic data reduction was carried out using Maxim DL 5.24 software (George 2000), and the bias, dark, and flat-field images followed the standard technique. We used SAO 106677 (R.A.: 314.0342, decl.: 19.8394) and SAO 89337 (RA.: 314.6170 and Dec.: 20.3980) as comparison stars. SAO 106663 (RA.: 313.8770 and Dec.: 19.6862) was also considered to be a check star. Also, the maximum apparent magnitude of the system's light curve was $V_{max} = 8.62(6)$ mag.

V997 Cyg was observed in a private observatory in Toulon, France, at a longitude of 05° 54′ 35″ E and a latitude of 43° 8′ 59″ N, and an altitude of 68 m above mean sea level. The observations were carried out on four nights from 2023 June to July. Observations employed an apochromatic refractor from TS Optics with a 102 mm aperture and a ZWO ASI 1600MM CCD. The binning of the images was 1×1, with a 180 s exposure time and the average temperature of the CCD was −15 °C. The basic data reduction was carried out by the bias, dark, and flat fields image and with the Siril 1.2.0-rc2 program. We used Gaia DR2 2137381511262134016 (R.A.: 296.9277 and decl.: 52.8988) and Gaia DR2 2137287331220260096 (R.A.: 296.8882 and dec.: 52.8103) as comparison and check stars, respectively. According to our observations, the light curve's maximum apparent magnitude was obtained to be $V_{max} = 13.19(9)$ mag.

TESS observed the LS Del (TIC 265972568) and V997 Cyg (TIC 27997238) binary systems. We used sector 55 with an exposure time of 120 seconds for the LS Del target system. For V997 Cyg, we used sectors 14 (1800 s exposure time), 15 (1800 s exposure time), 16 (1800 s exposure time), 41 (600 s exposure time), 54 (600 s exposure time), 55 (600 s exposure time), and 56 (200 s exposure time). The data are available at the Mikulski Archive for Space Telescopes (MAST).[15]

3. Orbital Period Variations

According to the ground-based observations for this study, we derived the primary and secondary times of minima. So, one primary and three secondary minima were extracted for the LS Del system, whereas for the V997 Cyg system, two primary and one secondary minima were extracted (Tables 1 and 2). Then, we performed an exhaustive search to find all times of minima reported in studies, databases, and catalogs. We obtained the data from the TESS observations and the American Association of Variable Star Observers (AAVSO), the All Sky Automated Survey (ASAS), the All Sky Automated Survey for SuperNovae (ASAS-SN), the Zwicky Transient Facility (ZTF), the Trans-Atlantic Exoplanet Survey (TrES), the Super Wide Angle Search for Planets (SWASP), and the Qatar Exoplanet Survey (QES) for both systems, and we used them to extract times of minima (Appendix Tables 6–7). The timing data used in the $O-C$ analysis of LS Del and V997 Cyg cover almost 48 and 61 yr, respectively. Then, using the reference ephemeris (Equations (1) and (2)), we calculated the epoch and $O-C$ values.

$$\begin{cases} \text{LS Del:} \\ \text{Min.}I\,(BJD_{\text{TDB}}) = 2442687.4185 + 0.3638404 \times E \\ \text{Bond (1976)} \end{cases} \quad (1)$$

[12] ASAS-SN Catalog of Variable Stars http://asas-sn.osu.edu/variables.
[13] The International Variable Star Index (VSX) https://www.aavso.org/vsx
[14] https://bsnp.info.
[15] https://mast.stsci.edu/portal/Mashup/Clients/Mast/Portal.htmL

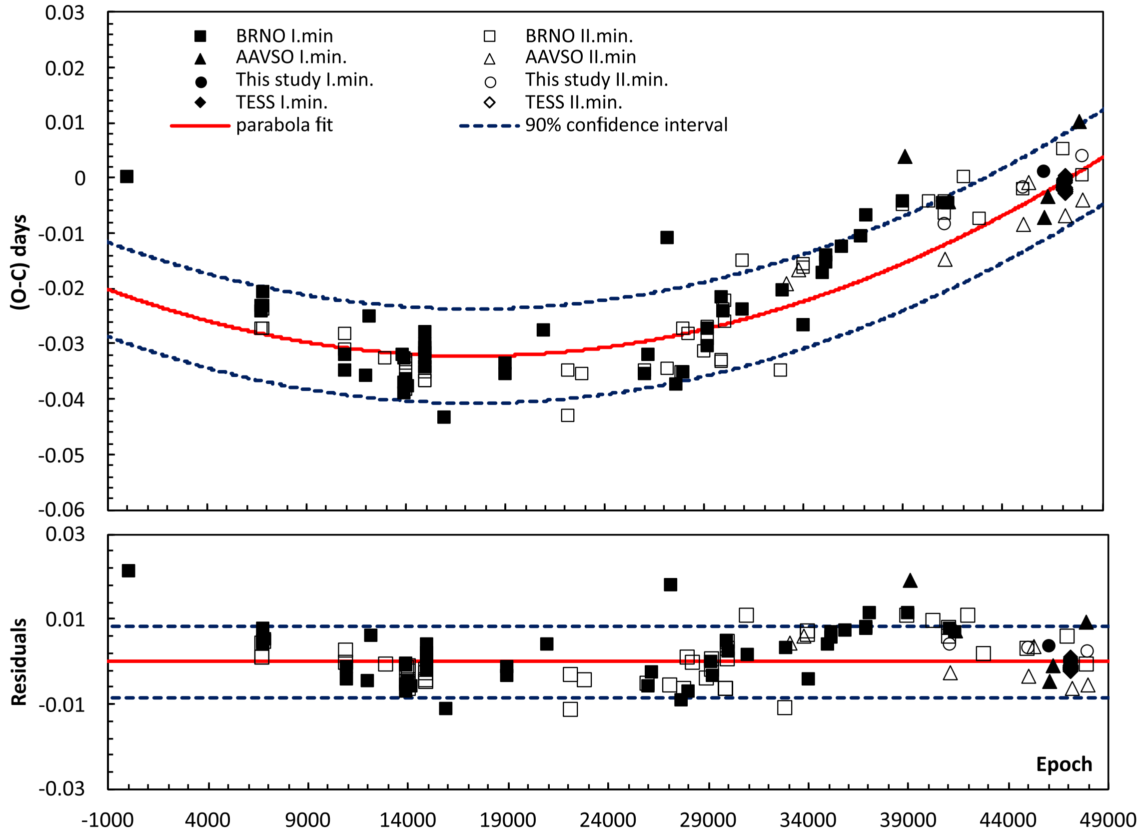

Figure 1. The $O-C$ diagram of LS Del with the parabolic fit to the $O-C$ data set is shown with a solid red line in the top panel. Residuals from the parabolic fit are displayed in the bottom panel of the diagram.

$$\begin{cases} V997\ \text{Cyg:} \\ \text{Min.}I\,(BJD_{\text{TDB}}) = 2455460.5143 + 0.458226 \times E \\ \text{Arenaetal. (2011)} \end{cases} \quad (2)$$

The $O-C$ diagrams of the LS Del and V997 Cyg systems and their corresponding residuals are presented in Figures 1 and 2 respectively. As shown in the $O-C$ diagrams of the target systems, both have an upward parabolic trend. We computed a new ephemeris for each of the systems (Equations (3) and (4))

$$\begin{cases} \text{LS Del:} \\ \text{Min.}I\,(BJD_{\text{TDB}}) = 2442687.3508(16) + 0.363841821(37) \times E \end{cases} \quad (3)$$

$$\begin{cases} V997\ \text{Cyg:} \\ \text{Min.}I\,(BJD_{\text{TDB}}) = 2455460.5144(1) + 0.458226914(17) \times E \end{cases} \quad (4)$$

where E is the cycle number after the reference cycle. Both target systems analyzed for orbital period changes in this work have observations over a long time. The $O-C$ parabolic variations suggest the orbital periods of LS Del and V997 Cyg systems are increasing at a rate of $dP/dt = 7.20 \times 10^{-08}$ days yr^{-1} and $dP/dt = 2.54 \times 10^{-08}$ days yr^{-1}, respectively.

Previous studies on the LS Del system have similarly indicated a tendency of changes with parabolic fit. The results of the Demircan et al. (1991) study displayed an increasing parabolic fit and the $O-C$ diagram indicates mass transfer from a less massive star to a more massive one. The Qian (2001) study also fit a parabolic trend on the $O-C$ diagram of LS Del and presented a continuous period increase rate of $dP/dt = 2.25 \times 10^{-07}$ days yr^{-1}.

We analyze the V997 Cyg system for the first time and the parabolic fit on the $O-C$ diagram can be considered based on the data. The parabolic fits for the LS Del and V997 Cyg systems could show star mass transfer in contact binary systems.

4. Light Curve Solutions

The LS Del and V997 Cyg systems' photometric light curve solutions were carried out using the PHysics Of Eclipsing BinariEs (PHOEBE) Python code version 2.4.9 (Prša et al. 2016; Conroy et al. 2020).

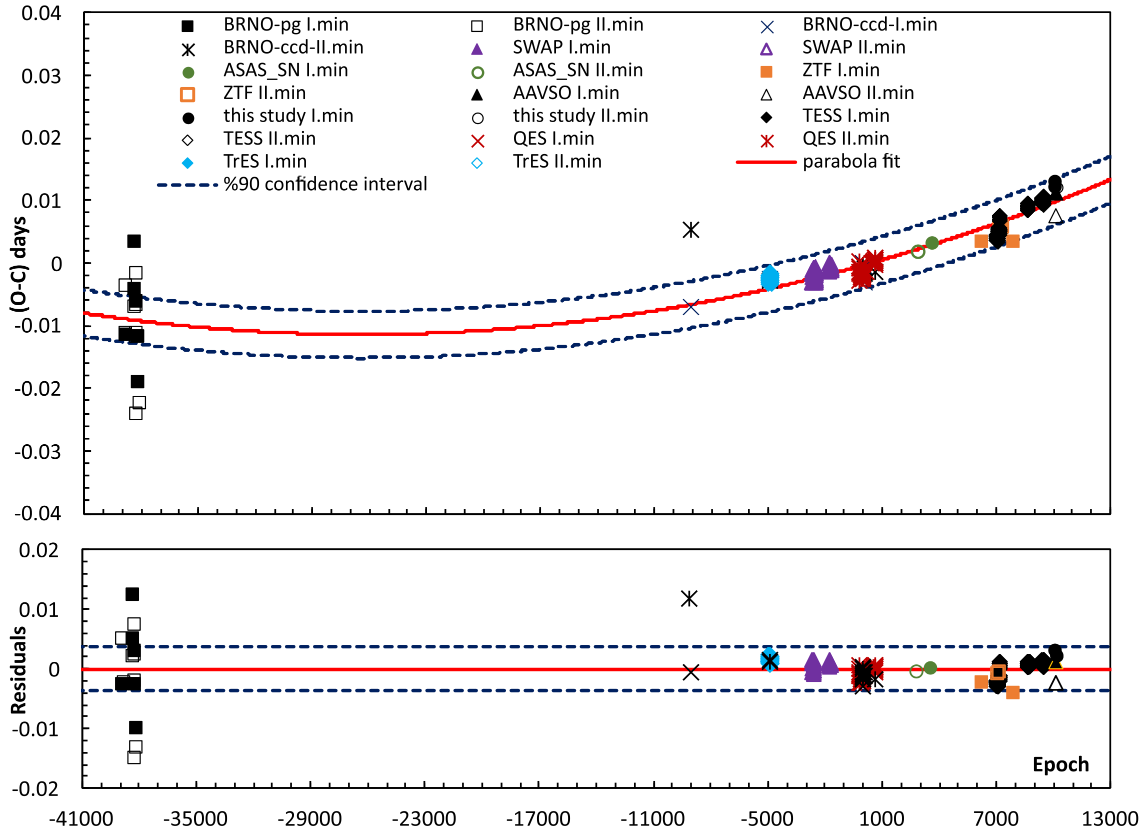

Figure 2. The V997 Cyg system's $O-C$ diagram. The solid red line in the top panel shows the parabolic fit to the $O-C$ data set. The diagram's bottom panel displays residuals of the fit.

We assumed the bolometric albedo and gravity-darkening coefficients were $A_1 = A_2 = 0.5$ (Ruciński 1969) and $g_1 = g_2 = 0.32$ (Lucy 1967), respectively. We modeled the stellar atmosphere using the Castelli & Kurucz (2004) method and the limb darkening coefficients were adopted as free parameters in the PHOEBE code. The reflection effect was also taken into account in our contact binary systems (e.g., Wilson 1990; Prša et al. 2016).

It should be mentioned that, regarding the use of TESS data for both systems, we only used one day of observations for each system. It appears that not all TESS data for all observation days can be used to provide an acceptable light curve analysis since the light curves will be thick. Thus, for LS Del and V997 Cyg, we utilized TESS data in sectors 55 and 56, respectively.

The initial system effective temperature from Gaia Data Release 3 (DR3) was taken into consideration and we set it on the hotter component. We used the depth difference between the light curve minima to estimate the temperature ratio. We set $q = 0.375$ for the LS Del system as an entitled value for the light curve analysis from the Lu & Rucinski (1999) and Deb & Singh (2011) studies. Also, considering that photometric data were available, the mass ratio of V997 Cyg was estimated using q-search. Then, following obtaining the temperatures, setting the mass ratio, and estimating the inclination and fillout factor, we attempted to obtain a good synthetic light curve.

Asymmetric maxima in the light curves of contact binary stars could be an indication of the well-known O'Connell effect (O'Connell 1951) and the presence of magnetic activity. The asymmetry in the LS Del system's light curve maxima indicates that a cold spot on the secondary star was required for the light curve's solution. It should be noted that the light curve analysis of the V997 Cyg system was performed without a starspot.

Finally, we employed PHOEBE's optimization tool to improve the output of light curve solutions and derive the final results. The results of the light curve analysis are shown in Table 3. The available results from other research that are comparable to the results of the current study are also included in Table 3. Figures 3 and 4 include the observational and synthetic light curves and the geometric structure of the systems in four phases. Also, the surface temperature of the stars are displayed in color (Figures 3 and 4); the brighter the color, the higher the temperature; also, the point of connection between the component stars has a lower temperature due to gravity darkening (Prša et al. 2016).

Table 1
Available Times of Minima for the LS Del System from the Literature and this Study

Min.(BJD_{TDB})	Epoch	$O-C$	Reference	Min.(BJD_{TDB})	Epoch	$O-C$	Reference
2442687.4185	0	0	Bond (1976)	2460081.5467	47807	0.0102	AAVSO
2445136.4051	6731	−0.0232	Sezer et al. (1984)	2460139.5651	47966.5	−0.0040	AAVSO
2445145.5001	6756	−0.0242	Sezer et al. (1984)	2447778.4186(16)	13992.5	−0.0367	Wieck & Wunder (1989)
2445146.4064	6758.5	−0.0275	Sezer et al. (1984)	2449588.3433(8)	18967	−0.0356	Demircan et al. (1994)
2445149.5059	6767	−0.0206	Sezer et al. (1984)	2449588.3458(7)	18967	−0.0336	Demircan et al. (1994)
2445150.4088	6769.5	−0.0273	Sezer et al. (1984)	2450301.4790(15)	20927	−0.0276	Selam et al. (1999)
2445177.3363	6843.5	−0.0240	Sezer et al. (1984)	2450731.3408(17)	22108.5	−0.0432	Selam et al. (1999)
2445177.5190	6844	−0.0232	Sezer et al. (1984)	2450758.2733(9)	22182.5	−0.0349	Selam et al. (1999)
2446668.1615	10941	−0.0348	Wang et al. (1987)	2452134.4990(2)	25965	−0.0355	Drozdz & Ogloza (2005)
2446670.1692	10946.5	−0.0283	Wang et al. (1987)	2452136.5007(2)	25970.5	−0.0349	Drozdz & Ogloza (2005)
2446671.0750	10949	−0.0321	Wang et al. (1987)	2452200.3577(2)	26146	−0.0320	Borkovits et al. (2002)
2447028.3626	11931	−0.0357	Wieck & Wunder (1989)	2452550.5516(2)	27108.5	−0.0345	Dvorak (2003)
2447114.2394	12167	−0.0253	Derman et al. (1991)	2452562.4001(3)	27141	−0.0108	Yilmaz et al. (2009)
2447386.5666	12915.5	−0.0326	Derman et al. (1991)	2452808.5138(10)	27817.5	−0.0351	Borkovits et al. (2004)
2447729.4866	13858	−0.0322	Wieck & Wunder (1989)	2452854.9032(11)	27945	−0.0353	Maciejewski & Karska (2004)
2447737.4906	13880	−0.0326	Wieck & Wunder (1989)	2452855.0932(21)	27945.5	−0.0273	Maciejewski & Karska (2004)
2447741.4865	13891	−0.0390	Derman et al. (1991)	2452952.6013(6)	28213.5	−0.0284	Dvorak (2004)
2447745.4906	13902	−0.0371	Derman et al. (1991)	2453229.4808(9)	28974.5	−0.0314	Biro et al. (2006)
2447772.4153	13976	−0.0366	Derman et al. (1991)	2453293.3390(3)	29150	−0.0272	Yilmaz et al. (2009)
2447778.4216	13992.5	−0.0337	Wieck & Wunder (1989)	2453302.2534(5)	29174.5	−0.0269	Albayrak et al. (2005)
2447790.4236	14025.5	−0.0384	Wieck & Wunder (1989)	2453303.3426(7)	29177.5	−0.0292	Albayrak et al. (2005)
2447790.4246	14025.5	−0.0374	Qian (2001)	2453304.2509(6)	29180	−0.0305	Albayrak et al. (2005)
2447790.4247	14025.5	−0.0373	Derman et al. (1991)	2453558.3909(5)	29878.5	−0.0331	Yilmaz et al. (2009)
2447790.4253	14025.5	−0.0367	Derman et al. (1991)	2453559.4822(4)	29881.5	−0.0333	Biro et al. (2006)
2447790.4276	14025.5	−0.0345	Demircan et al. (1991)	2453560.4034(4)	29884	−0.0217	Yilmaz et al. (2009)
2447790.4290	14025.5	−0.0330	Kreiner et al. (2001) [a]	2453589.3266(6)	29963.5	−0.0238	Yilmaz et al. (2009)
2447822.2602	14113	−0.0379	Derman et al. (1991)	2453589.5082(9)	29964	−0.0241	Yilmaz et al. (2009)
2448119.5214	14930	−0.0343	Demircan et al. (1991)	2453606.4247(8)	30010.5	−0.0262	Yilmaz et al. (2009)
2448119.5277	14930	−0.0280	Demircan et al. (1991)	2453613.3417(4)	30029.5	−0.0222	Albayrak et al. (2005)
2448122.4337	14938	−0.0328	Demircan et al. (1991)	2453937.5308(3)	30920.5	−0.0149	Biro et al. (2007)
2448122.4358	14938	−0.0307	Demircan et al. (1991)	2453938.4313(3)	30923	−0.0240	Biro et al. (2007)
2448123.3392	14940.5	−0.0369	Demircan et al. (1991)	2454628.8075(10)	32820.5	−0.0348	Deb & Singh (2011)
2448123.3409	14940.5	−0.0352	Demircan et al. (1991)	2454650.4706(5)	32880	−0.0202	Parimucha et al. (2009)
2448129.3476	14957	−0.0318	Demircan et al. (1991)	2455050.5171(7)	33979.5	−0.0163	Hubscher et al. (2010)
2448129.3492	14957	−0.0302	Demircan et al. (1991)	2455059.4209(6)	34004	−0.0265	Hubscher et al. (2010)
2448131.3438	14962.5	−0.0368	Demircan et al. (1991)	2455059.6138(7)	34004.5	−0.0156	Hubscher et al. (2010)
2448131.3464	14962.5	−0.0342	Demircan et al. (1991)	2455401.4402(8)	34944	−0.0172	Parimucha et al. (2011)
2448472.4375	15900	−0.0434	Muyesseroglu & Selam (1994)	2455463.2950(8)	35114	−0.0153	Parimucha et al. (2011)
2449588.3438	18967	−0.0356	Heckert (1994)	2455476.3944(6)	35150	−0.0141	Parimucha et al. (2011)
2449588.3458	18967	−0.0336	Heckert (1994)	2455735.4505(3)	35862	−0.0125	Parimucha et al. (2013)
2451000.2264	22847.5	−0.0357	Kiss et al. (1999)	2456105.4780(12)	36879	−0.0107	Parimucha et al. (2013)
2452734.8338	27615	−0.0374	ASAS	2456105.4781(6)	36879	−0.0106	Parimucha et al. (2013)
2454722.6942	33078.5	−0.0190	AAVSO	2456180.4329(4)	37085	−0.0069	Parimucha et al. (2013)
2454947.9139	33697.5	−0.0165	AAVSO	2456852.8127(7)	38933	−0.0041	Nelson (2015)
2456898.6645	39059	0.0038	AAVSO	2456866.8198(7)	38971.5	−0.0049	Nelson (2015)
2457608.5087	41010	−0.0046	BRNO	2457329.6255(3)	40243.5	−0.0042	Samolyk (2016)
2457613.4106	41023.5	−0.0146	AAVSO	2457 613.4169(4)	41023.5	−0.0082	This study
2457636.7068	41087.5	−0.0042	Samolyk (2017)	2457974.3548(4)	42015.5	0.0000	Ozavci et al. (2019)
2457704.5625	41274	−0.0047	BRNO	2458262.5091(1)	42807.5	−0.0073	Ozavci et al. (2019)
2457704.5628	41274	−0.0044	AAVSO	2459049.5012(9)	44970.5	−0.0021	Samolyk (2020)
2459146.6477	45237.5	−0.0009	AAVSO	2459049.5016(5)	44970.5	−0.0017	This study
2459502.6631	46216	−0.0033	AAVSO	2459440.4508(3)	46045	0.0011	This study
2459784.4660	46990.5	0.0051	AAVSO	2460139.5730(4)	47966.5	0.0040	This study
2459826.6594	47106.5	−0.0069	AAVSO	…	…	…	…

Note.
[a] http://www.as.wsp.krakow.pl/o-c

Table 2
Available Times of Minima for the V997 Cyg System from the Literature and this Study

Min.($BJD_{\rm TDB}$)	Epoch	$O-C$	Reference	Min.($BJD_{\rm TDB}$)	Epoch	$O-C$	Reference
2437668.2734	−38828.5	−0.0126	BRNO	2455462.3453(7)	4	−0.0019	Arena et al. (2011)
2437669.3934	−38826	−0.0382	BRNO	2455463.4925(12)	6.5	−0.0003	Arena et al. (2011)
2437696.6584	−38766.5	−0.0376	BRNO	2455469.4482(4)	19.5	−0.0015	Arena et al. (2011)
2437903.5714	−38315	−0.0137	BRNO	2455469.4489(17)	19.5	−0.0008	Arena et al. (2011)
2437904.5124	−38313	0.0109	BRNO	2455472.4251(20)	26	−0.0031	Arena et al. (2011)
2437906.5404	−38308.5	−0.0232	BRNO	2455476.3215(22)	34.5	−0.0016	Arena et al. (2011)
2437933.5614	−38249.5	−0.0375	BRNO	2455478.3844(11)	39	−0.0007	Arena et al. (2011)
2437934.5094	−38247.5	−0.0059	BRNO	2455479.3002(4)	41	−0.0014	Arena et al. (2011)
2437939.5334	−38236.5	−0.0224	BRNO	2455764.5457(5)	663.5	−0.0015	Banfi et al. (2012)
2437940.4334	−38234.5	−0.0389	BRNO	2456785.0182	2890.5	0.0017	ASAS-SN
2437944.5154	−38225.5	−0.0809	BRNO	2457121.1283	3624	0.0030	ASAS-SN
2437947.5544	−38219	−0.0204	BRNO	2458336.8021	6277	0.0032	ZTF
2437959.4494	−38193	−0.0393	BRNO	2458723.7764	7121.5	0.0057	ZTF
2437970.4224	−38169	−0.0637	BRNO	2458763.6423	7208.5	0.0060	ZTF
2438001.3414	−38101.5	−0.0749	BRNO	2459082.7941	7905	0.0033	ZTF
2451291.8085(22)	−9097.5	0.0053	Diethelm (2001)	2460118.3926	10165	0.0111	AAVSO
2451304.8555(27)	−9069	−0.0071	Diethelm (2001)	2460118.3945(7)	10165	0.0129	This study
2453210.1638	−4911	−0.0026	BRNO	2460118.6182	10165.5	0.0075	AAVSO
2453210.3928	−4910.5	−0.0027	BRNO	2460123.4340(20)	10176	0.0120	This study
2455459.3675(14)	−2.5	−0.0012	Arena et al. (2011)	2460130.5365(8)	10191.5	0.0120	This study
2455460.5143(17)	0	0	Arena et al. (2011)	…	…	…	…

Table 3
Photometric Solutions of the LS Del and V997 Cyg Binary Systems

Parameter	LS Del				V997 Cyg
	This Study	Maceroni & van't Veer (1996)	Lu & Rucinski (1999)	Deb & Singh (2011)	
T_1 (K)	6021(37)	5704	…	6250(185)	6629(38)
T_2 (K)	5959(35)	5780	…	6192(168)	6569(39)
$q=M_2/M_1$	0.407(50)	0.562	0.375(10)	0.375(10)	1.078(58)
i°	47.81(75)	48.5	48.5	45.25(2.45)	70.38(25)
f	0.106(31)	0.06	0.07	0.09	0.117(18)
$\Omega_1=\Omega_2$	2.666(45)	…	…	6.051(80)	3.811(32)
$l_1/l_{\rm tot}(V)$	0.699(32)	…	…	…	0.494(12)
$l_2/l_{\rm tot}(V)$	0.301(32)	…	…	…	0.506(12)
$l_1/l_{\rm tot}(TESS)$	0.701(32)	…	…	…	…
$l_2/l_{\rm tot}(TESS)$	0.299(32)	…	…	…	…
$r_{1({\rm mean})}$	0.468(11)	0.429	…	0.308(9)	0.385(5)
$r_{2({\rm mean})}$	0.311(10)	0.328	…	0.478(8)	0.398(5)
Phase shift	0.0001(1)	…	…	…	0.025(1)
Col.(deg)	83	…	…	…	…
Long.(deg)	56	…	…	…	…
Rad.(deg)	24	…	…	…	…
$T_{\rm spot}/T_{\rm star}$	0.86	…	…	…	…
Component	Secondary	…	…	…	…

5. Absolute Parameters

There are various methods for estimating absolute parameters. Some of them can be estimated using empirical or statistical relationships between parameters, while one provides an estimate of the absolute parameters by utilizing Gaia's parallax. Gaia DR3's parallax is accurate enough to be used in computations (Li et al. 2021). This method of determining absolute parameters makes use of the light curve solution, and is capable of obtaining orbital period and observational results. Thus, the absolute magnitude of the system can be determined

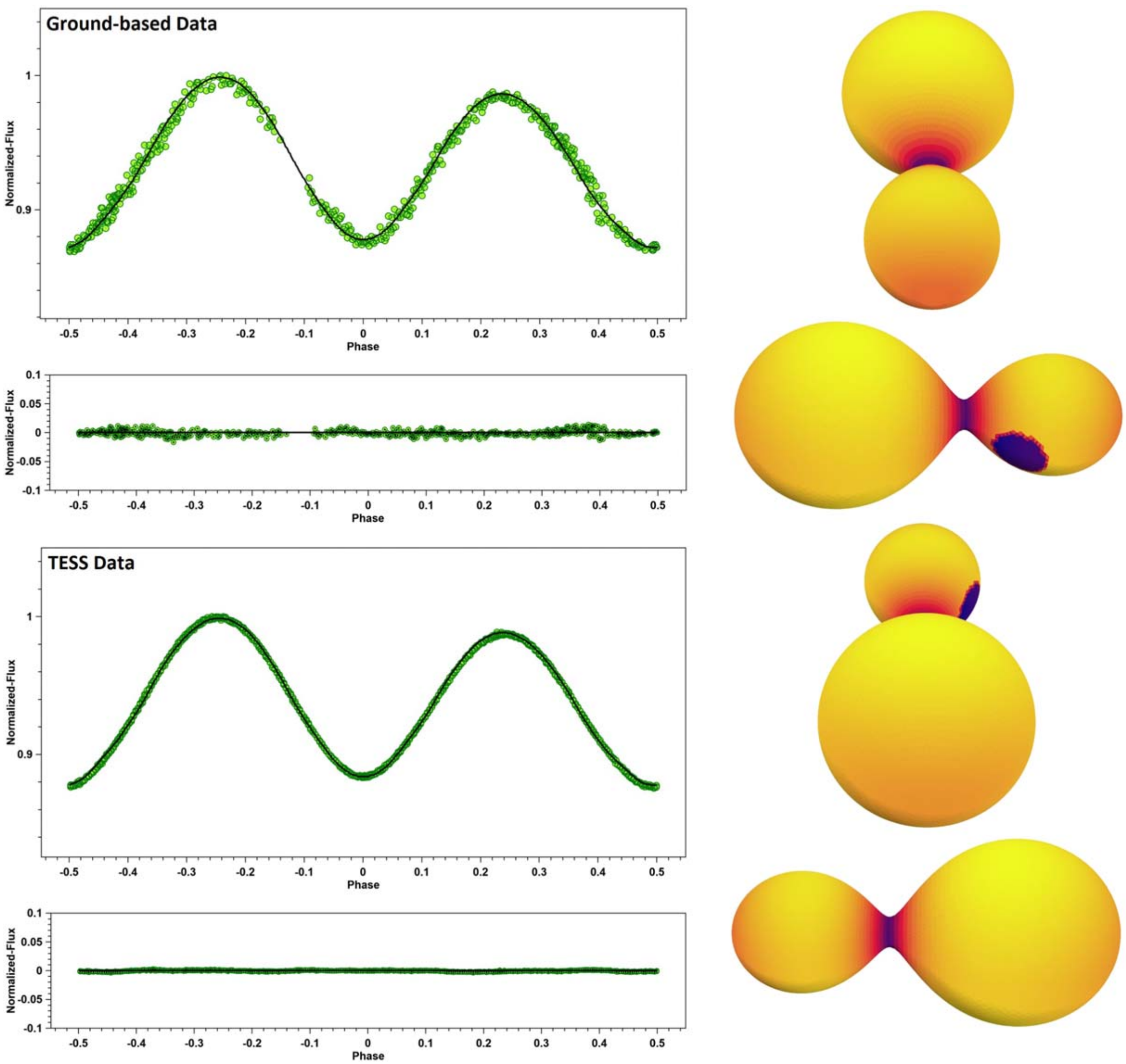

Figure 3. Observational (TESS and ground-based) and synthetic light curves, along with the three-dimensional view in four phases of the LS Del system. The green points are the data and the black line is the synthetic fit.

using the extinction coefficient A_V from the Green et al. (2019) study, and $V_{\max}$, and distance. Next, $M_{V_{1,2}}$ values are computed using $l_{1,2}/l_{\rm tot}$ from the light curve solution. We could then estimate each star's absolute bolometric value using the Bolometric Correction (BC) from the Flower (1996) study. The radius of a star can be calculated from its luminosity and effective temperature applying well-known equations in stellar astrophysics. Also, when we have $r_{{\rm mean}_{1,2}}$, a_1 and a_2 can be calculated. It can be inferred that the light curve analysis is appropriate if the values of a_1 and a_2 are close to each other. We can employ the average of a_1 and a_2 to determine $a(R_\odot)$. Finally, by using the orbital period and the mass ratio, the mass of each star is estimated from Kepler's third law equation. This is the method and process we used to estimate the absolute parameters of both systems which are presented in Table 4 under the title Method 1.

We also estimated the absolute parameters of the LS Del and V997 Cyg systems using the $M_1 - P$ relationship (Model 2 in Table 5) from the Latković et al. (2021) study.

$$M_1 = (2.94 \pm 0.21)P + (0.16 \pm 0.08) \quad (5)$$

Then, considering the mass ratio, the mass of the other component can be calculated. We estimated the value of $a(R_\odot)$ using Kepler's third law, and then employed the well-known $R = a \times r_{({\rm mean}1,2)}$ relation to find the star's radius. The luminosity can be computed using the temperature and radius of the stars, and the absolute bolometric value is then able to be

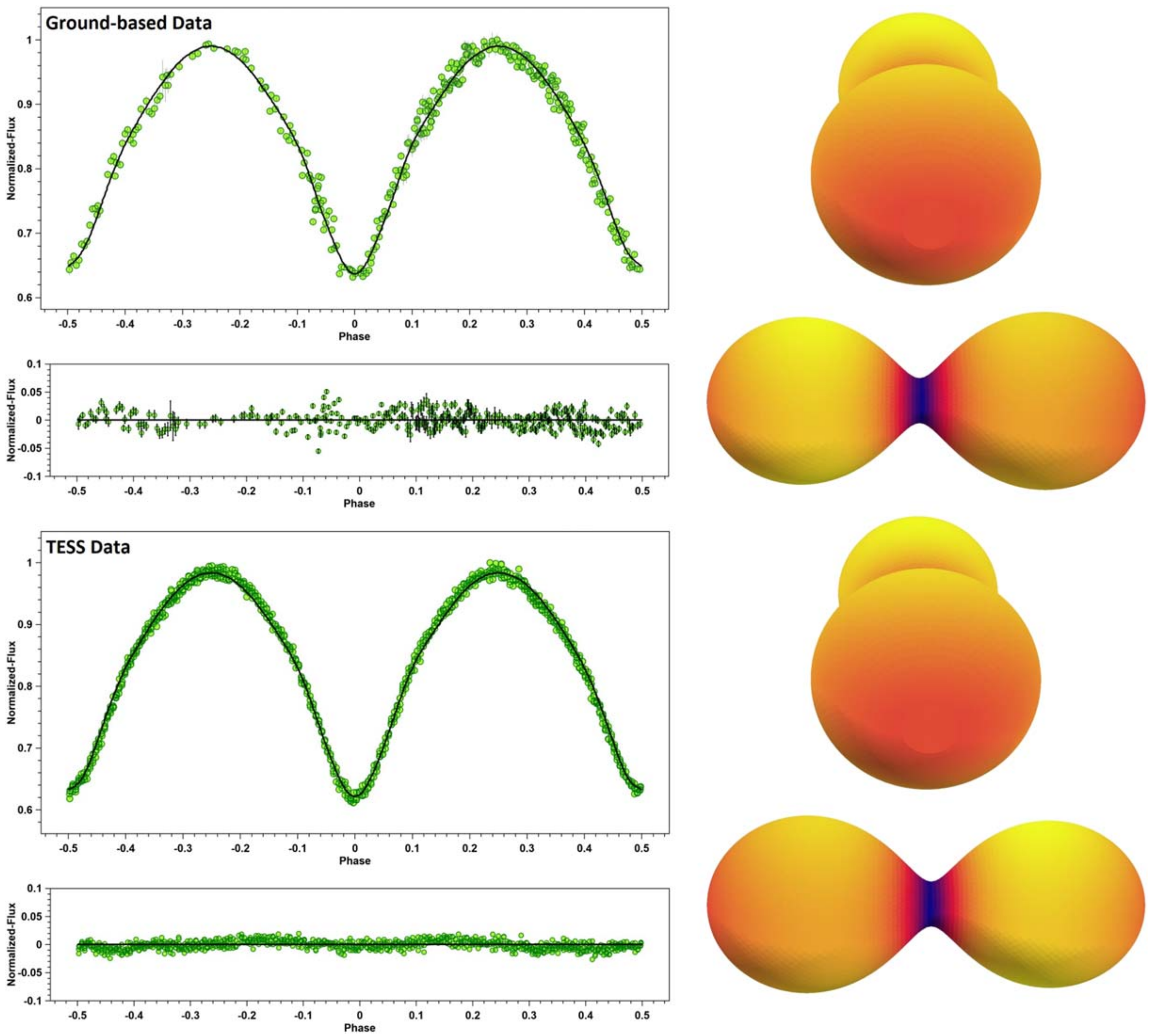

Figure 4. Observational (TESS and ground-based) and synthetic light curves, as well as the three-dimensional view in four phases of the V997 Cyg binary system. The data are displayed by the green dots, while the synthetic fit is shown by the black line.

determined for each star. These solutions are presented in Table 4 under the title Method 2.

6. Discussion and Conclusion

Photometric observations were conducted with a *V* filter at two French observatories targeting the LS Del and V997 Cyg systems. Following the standard method, data reduction processes were carried out, and light curves were prepared for analysis. Additionally, TESS data were used for both binary systems in this work. The following conclusions can be derived based on the results of our investigation:

(A) Light curve analyses were performed using PHOEBE Python code. We have performed the light curve solution for the LS Del and V997 Cyg systems, and for LS Del it is necessary to add a cold starspot. The obtained mass ratio is in good agreement with other studies (Table 3). The effective temperature difference between the two stars in the LS Del system is 62 K, and in the V997 Cyg system, it is 60 K. According to the temperature obtained in the light curve solutions, it is possible to obtain the spectral category of each star using studies Cox (2020) and Eker et al. (2018): For the LS Del system, star1 is G0 and star2 is G1, while both stars of V997 Cyg are F3.

(B) As explained in Section 5, we have used two methods to estimate the absolute parameters: Method 1 is based on the Gaia DR3 parallax, and Method 2 uses a relationship between mass and orbital period.

The main method we have chosen for this study is to use Gaia DR3 parallax. The accuracy of this method depends on some parameters, especially Gaia DR3 parallax, A_V, $V_{\max}$, and

Table 4
The Absolute Parameter Estimation

Parameter	LS Del				V997 Cyg			
	Method 1		Method 2		Method 1		Method 2	
	Star1	Star2	Star1	Star2	Star1	Star2	Star1	Star2
$M(M_\odot)$	1.768(114)	0.719(46)	1.230(156)	0.501(133)	2.255(276)	2.431(298)	1.507(176)	1.625(286)
$R(R_\odot)$	1.352(29)	0.909(9)	1.205(193)	0.801(136)	1.595(86)	1.683(90)	1.409(283)	1.456(292)
$L(L_\odot)$	2.154(42)	0.934(39)	1.720(652)	0.729(292)	4.406(382)	4.734(394)	3.454(1.639)	3.559(1.693)
$M_{\rm bol}$(mag.)	3.907(21)	4.814(46)	4.141(349)	5.074(366)	3.310(92)	3.052(93)	3.384(422)	3.352(422)
$log(g)$(cgs)	4.424(10)	4.378(37)	4.366(77)	4.330(34)	4.386(100)	4.372(101)	4.318(111)	4.322(88)
$a(R_\odot)$	2.906(62)		2.575(344)		4.186(172)		3.659(679)	

light curve solution results. We calculated A_V using the dust-maps Python package of Green et al. (2019). The results show LS Del and V997 Cyg have A_V of 0.061(1) and 0.405(1), respectively. According to the A_V, we can trust estimating absolute parameters using Gaia DR3 parallax for LS Del (Method 1). However, for V997 Cyg with a slightly inappropriate value, we preferred to use Method 2 (Poro et al. 2024a).

(C) We gathered all the times of minima that could be found in the literature and also extracted minima from our observations and space-based data. Based on reference ephemeris, we calculated epochs and $O-C$ values and presented a new ephemeris for each system. The $O-C$ diagrams for both systems show a parabolic fit with an upward trend. Also, we calculated orbital period increase rate for each system, which shows the less massive star is transferring mass to the more massive one. The following Equation (6) was used to calculate the quantity of mass transferred from the orbital period change

$$\frac{\Delta P}{P} = 3\Delta M\frac{M_1 - M_2}{M_1 M_2} \tag{6}$$

Taking into account the system elements and M_1 and M_2 from Table 4, we obtain a mass transfer rate for the LS Del system of $dM/dt = -1.96 \times 10^{-7}$ $M_\odot$ yr^{-1}, and $dM/dt = -3.83 \times 10^{-7}$ $M_\odot$ yr^{-1} for V997 Cyg.

The main causes of orbital period variation in binary stars include apsidal motion, magnetic activity, the third-body effect, mass, and angular momentum transfer and loss (Soomandar & Poro 2024). The residual panel in Figure 1 for LS Del shows the possibility of a sinusoidal trend. This becomes significant when the TESS information indicates a possible candidate for the third body in the LS Del system. Therefore, we performed a fit based on the trend in the residuals and the presence of a third body (Figure 5). Also, we calculated the possible third body parameters (Table 5). As can be seen in the residuals of Figure 5, even another specific trend can be understood. It suggests long-term spectroscopic observations of the LS Del system need to be considered in the future.

Table 5
Parameters and their Errors Obtained from $O-C$ Analysis for LS Del, Considering the Third Body Probability

Parameter	Result
$T_0(BJD_{\rm TDB})$	2442 687.4183
$P_{\rm orb}$(day)	0.363 840 4
Q(day)	$(0.0166 \pm 0.0003) \times 10^{-10}$
$a_{12}sini_3$(AB)	6.8917 ± 0.4248
A_s(day)	0.03979 ± 0.00440
e'	0.7966 ± 0.2157
ω'	271.2 ± 7.7
$T_3(BJD_{\rm TDB})$	$3\,027\,714 \pm 981$
P_3(yr)	263.7 ± 0.3
$f(M_3)(M_\odot)$	0.0047 ± 0.0003
$(M_3)(M_\odot)$ for $i = 90°$	0.29

The results of TESS sector 55, available in the MAST portal and published in PDF format, consider the third object as a planet candidate. TESS reported the temperature of the third object to be $T_{eq} = 3170(122)$ K and $T_p = 3818(468)$ K. It seems this third body, with the mass of $0.29 M_\odot$ estimated by this study, can be assumed to be an M-type dwarf star. The temperature reported by TESS and the third body mass can be considered consistent with each other, according to studies Pecaut & Mamajek (2013), Cifuentes et al. (2020), and Mamajek (2022).[16] As mentioned, we suggest that the fourth body in this system should be investigated in the future.

(D) The log-scale Mass-Luminosity ($M-L$) and Mass-Radius ($M-R$) diagrams (Figure 6(a) and (b)) illustrate the target systems' evolutionary stage based on the estimated absolute parameters. Figure 6(a) and (b) shows the positions of the primary and secondary components as well as the theoretical Zero-Age Main Sequence (ZAMS) and Terminal-Age Main Sequence (TAMS) lines. Figure 6(c) displays the systems' positions on the $q-L_{\rm ratio}$ relationship, which is in

[16] https://www.pas.rochester.edu/~emamajek/EEM_dwarf_UBVIJHK_colors_Teff.txt

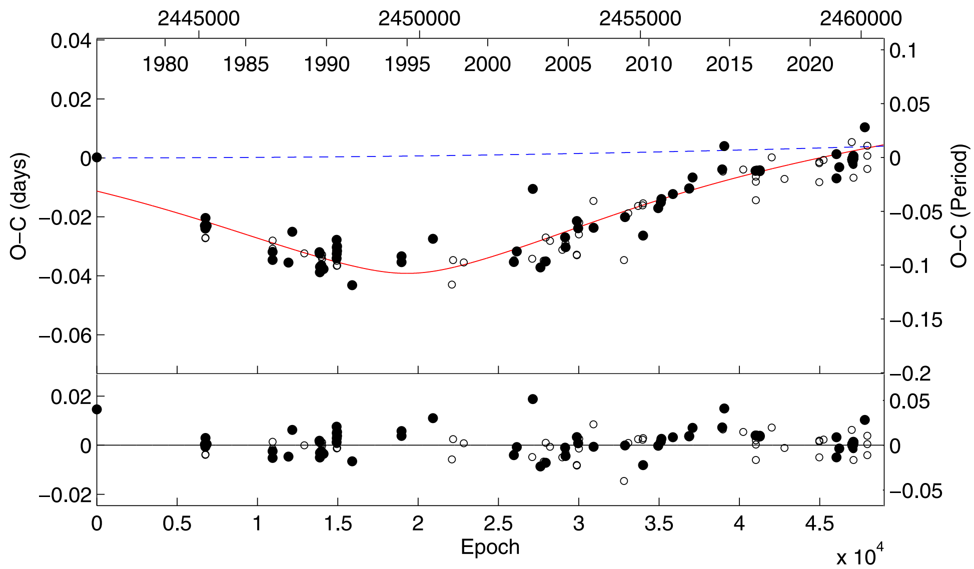

Figure 5. $O-C$ diagram considering the possibility of the presence of a third body in the LS Del system.

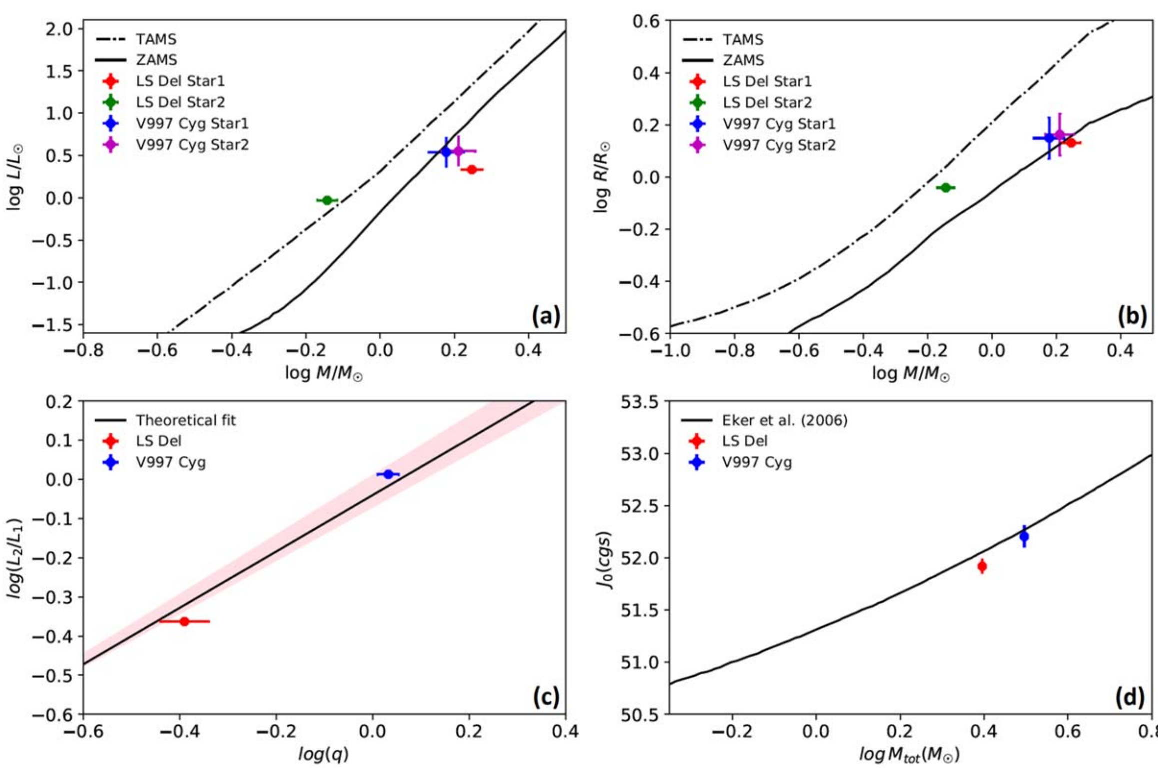

Figure 6. The $M-L$, $M-R$, $q-L_{\rm ratio}$, and $M_{\rm tot}-logJ_0$ diagrams.

good agreement with the model provided by Poro et al. (2024b).

We calculated the orbital angular momentum (J_0) of the systems based on Equation (7) presented by the Eker et al. (2006) study.

$$J_0 = \frac{q}{(1+q)^2}\sqrt[3]{\frac{G^2}{2\pi}M^5 P} \tag{7}$$

The results show that $\log J_0$ values for LS Del and V997 Cyg are 51.919(65) and 52.204(98), respectively. The parabolic boundary in Figure 6(d) is related to the Poro et al. (2024b) study, which indicates that both of our target systems are in the region of contact binary systems.

Acknowledgments

This manuscript was prepared by the BSN project (https://bsnp.info/). This project was supported by the Scientific Research Projects Coordination Unit of Erciyes University (project number FBA-2022-11737). We have made use of data from the European Space Agency (ESA) mission Gaia (http://www.cosmos.esa.int/gaia), processed by the Gaia Data Processing and Analysis Consortium (DPAC). This work includes data from the TESS mission observations. Funding for the TESS mission is provided by the NASA Explorer Program. We thank Ehsan Paki for his comments on the orbital period variation section.

Data Availability

Ground-based data will be made available on request.

Appendix

The appendix tables list the extracted times of minima for LS Del and V997 Cyg using space-based data. They display the times of minima in the first column, the epochs in the second column, the $O-C$ values in the third column, and the references in the fourth column. The minimum time error in all appendix tables is 0.0001. All times of minima in the appendix tables are in $BJD_{\rm TDB}$.

Table 6
Extracted Times of Minima of the LS Del Binary System from TESS Data

Min.	Epoch	$O-C$	Reference	Min.	Epoch	$O-C$	Reference	Min.	Epoch	$O-C$	Reference
2459797.1937	47025.5	−0.0015	TESS	2459805.9255	47049.5	−0.0020	TESS	2459815.7488	47076.5	−0.0023	TESS
2459797.3763	47026	−0.0009	TESS	2459806.1087	47050	−0.0006	TESS	2459815.9326	47077	−0.0004	TESS
2459797.5574	47026.5	−0.0017	TESS	2459806.2893	47050.5	−0.0020	TESS	2459816.1128	47077.5	−0.0022	TESS
2459797.7402	47027	−0.0008	TESS	2459806.4726	47051	−0.0005	TESS	2459816.2962	47078	−0.0007	TESS
2459797.9214	47027.5	−0.0015	TESS	2459806.6530	47051.5	−0.0022	TESS	2459816.4764	47078.5	−0.0024	TESS
2459798.1042	47028	−0.0006	TESS	2459806.8365	47052	−0.0006	TESS	2459816.6601	47079	−0.0006	TESS
2459798.2850	47028.5	−0.0017	TESS	2459807.0171	47052.5	−0.0019	TESS	2459816.8405	47079.5	−0.0022	TESS
2459798.4676	47029	−0.0011	TESS	2459807.2003	47053	−0.0005	TESS	2459817.0238	47080	−0.0007	TESS
2459798.6489	47029.5	−0.0018	TESS	2459807.3808	47053.5	−0.0020	TESS	2459817.2041	47080.5	−0.0024	TESS
2459798.8316	47030	−0.0009	TESS	2459807.5641	47054	−0.0006	TESS	2459817.3878	47081	−0.0006	TESS
2459799.0125	47030.5	−0.0020	TESS	2459807.7446	47054.5	−0.0020	TESS	2459817.5679	47081.5	−0.0024	TESS
2459799.1957	47031	−0.0006	TESS	2459808.1086	47055.5	−0.0018	TESS	2459817.7518	47082	−0.0005	TESS
2459799.3765	47031.5	−0.0019	TESS	2459808.2916	47056	−0.0008	TESS	2459817.9318	47082.5	−0.0024	TESS
2459799.5597	47032	−0.0005	TESS	2459808.4725	47056.5	−0.0018	TESS	2459818.1156	47083	−0.0005	TESS
2459799.7402	47032.5	−0.0020	TESS	2459808.6557	47057	−0.0005	TESS	2459818.2956	47083.5	−0.0024	TESS
2459799.9234	47033	−0.0007	TESS	2459808.8362	47057.5	−0.0020	TESS	2459818.4796	47084	−0.0004	TESS
2459800.1038	47033.5	−0.0022	TESS	2459809.0195	47058	−0.0006	TESS	2459818.6594	47084.5	−0.0024	TESS
2459800.2872	47034	−0.0007	TESS	2459809.2001	47058.5	−0.0019	TESS	2459818.8437	47085	−0.0001	TESS
2459800.4679	47034.5	−0.0019	TESS	2459809.3833	47059	−0.0006	TESS	2459819.0233	47085.5	−0.0024	TESS
2459800.6511	47035	−0.0006	TESS	2459809.5641	47059.5	−0.0017	TESS	2459819.2075	47086	−0.0001	TESS
2459800.8315	47035.5	−0.0021	TESS	2459809.7475	47060	−0.0003	TESS	2459819.3870	47086.5	−0.0025	TESS
2459801.0147	47036	−0.0008	TESS	2459809.9279	47060.5	−0.0018	TESS	2459819.5711	47087	−0.0003	TESS
2459801.1955	47036.5	−0.0020	TESS	2459811.0196	47063.5	−0.0016	TESS	2459819.7508	47087.5	−0.0026	TESS
2459801.3784	47037	−0.0010	TESS	2459811.2026	47064	−0.0005	TESS	2459819.9352	47088	−0.0001	TESS
2459801.5594	47037.5	−0.0020	TESS	2459811.3834	47064.5	−0.0016	TESS	2459820.1149	47088.5	−0.0023	TESS
2459801.7424	47038	−0.0009	TESS	2459811.5665	47065	−0.0005	TESS	2459820.2992	47089	0.0000	TESS
2459801.9231	47038.5	−0.0021	TESS	2459811.7470	47065.5	−0.0019	TESS	2459820.4786	47089.5	−0.0024	TESS
2459802.1063	47039	−0.0008	TESS	2459811.9302	47066	−0.0006	TESS	2459820.6631	47090	0.0001	TESS
2459802.2871	47039.5	−0.0020	TESS	2459812.1107	47066.5	−0.0020	TESS	2459820.8425	47090.5	−0.0024	TESS
2459802.4702	47040	−0.0008	TESS	2459812.2939	47067	−0.0008	TESS	2459821.0269	47091	0.0000	TESS
2459802.6508	47040.5	−0.0021	TESS	2459812.4746	47067.5	−0.0019	TESS	2459821.2066	47091.5	−0.0021	TESS
2459802.8341	47041	−0.0007	TESS	2459812.6578	47068	−0.0007	TESS	2459821.3911	47092	0.0005	TESS
2459803.0147	47041.5	−0.0020	TESS	2459812.8383	47068.5	−0.0021	TESS	2459821.5702	47092.5	−0.0024	TESS
2459803.1979	47042	−0.0007	TESS	2459813.0219	47069	−0.0004	TESS	2459821.7548	47093	0.0003	TESS
2459803.3786	47042.5	−0.0020	TESS	2459813.2019	47069.5	−0.0023	TESS	2459821.9341	47093.5	−0.0023	TESS
2459803.5618	47043	−0.0007	TESS	2459813.3858	47070	−0.0003	TESS	2459822.1185	47094	0.0002	TESS
2459803.7425	47043.5	−0.0019	TESS	2459813.5659	47070.5	−0.0022	TESS	2459822.2979	47094.5	−0.0024	TESS
2459803.9258	47044	−0.0005	TESS	2459813.7495	47071	−0.0005	TESS	2459822.4825	47095	0.0004	TESS
2459804.1063	47044.5	−0.0019	TESS	2459813.9300	47071.5	−0.0020	TESS	2459822.6618	47095.5	−0.0023	TESS
2459804.2896	47045	−0.0005	TESS	2459814.1134	47072	−0.0004	TESS	2459822.8461	47096	0.0001	TESS
2459804.4701	47045.5	−0.0019	TESS	2459814.2937	47072.5	−0.0021	TESS	2459823.0256	47096.5	−0.0024	TESS
2459804.6536	47046	−0.0004	TESS	2459814.4771	47073	−0.0006	TESS	2459823.2097	47097	−0.0001	TESS
2459804.8338	47046.5	−0.0021	TESS	2459814.6574	47073.5	−0.0022	TESS	2459823.3892	47097.5	−0.0026	TESS
2459805.0174	47047	−0.0005	TESS	2459814.8410	47074	−0.0005	TESS	2459823.5738	47098	0.0001	TESS
2459805.1976	47047.5	−0.0021	TESS	2459815.0214	47074.5	−0.0020	TESS	2459823.7534	47098.5	−0.0023	TESS
2459805.3810	47048	−0.0007	TESS	2459815.2047	47075	−0.0007	TESS	2459823.9378	47099	0.0003	TESS
2459805.5618	47048.5	−0.0018	TESS	2459815.3851	47075.5	−0.0021	TESS	2459824.1169	47099.5	−0.0025	TESS
2459805.7449	47049	−0.0006	TESS	2459815.5687	47076	−0.0005	TESS				

Table 7
Extracted Times of Minima of the V997 Cyg Binary System from Space-based Data

Min.	Epoch	$O-C$	Reference	Min.	Epoch	$O-C$	Reference	Min.	Epoch	$O-C$	Reference
2453170.7566	−4997	−0.0023	TrES	2453239.9493	−4846	−0.0018	TrES	2454638.6858	−1793.5	−0.0001	SWASP
2453171.9015	−4994.5	−0.0030	TrES	2453240.8653	−4844	−0.0022	TrES	2454644.6422	−1780.5	−0.0006	SWASP
2453172.8180	−4992.5	−0.0029	TrES	2453241.7810	−4842	−0.0029	TrES	2454645.5583	−1778.5	−0.0010	SWASP
2453173.9643	−4990	−0.0022	TrES	2453242.6975	−4840	−0.0029	TrES	2454646.7041	−1776	−0.0008	SWASP
2453174.8797	−4988	−0.0033	TrES	2453242.9265	−4839.5	−0.0031	TrES	2454647.6203	−1774	−0.0011	SWASP
2453175.7975	−4986	−0.0019	TrES	2453243.8440	−4837.5	−0.0020	TrES	2454662.5127	−1741.5	−0.0010	SWASP
2453176.7130	−4984	−0.0029	TrES	2453244.7604	−4835.5	−0.0021	TrES	2454668.4694	−1728.5	−0.0012	SWASP
2453176.9420	−4983.5	−0.0030	TrES	2453245.6765	−4833.5	−0.0024	TrES	2454669.6153	−1726	−0.0009	SWASP
2453177.8588	−4981.5	−0.0026	TrES	2453245.9058	−4833	−0.0022	TrES	2454670.5316	−1724	−0.0010	SWASP
2453178.7757	−4979.5	−0.0022	TrES	2453246.8224	−4831	−0.0021	TrES	2454672.5945	−1719.5	−0.0002	SWASP
2453179.6919	−4977.5	−0.0024	TrES	2453247.7390	−4829	−0.0019	TrES	2454684.5076	−1693.5	−0.0009	SWASP
2453180.8379	−4975	−0.0021	TrES	2453248.6545	−4827	−0.0029	TrES	2454688.4025	−1685	−0.0009	SWASP
2453181.7541	−4973	−0.0022	TrES	2453248.8835	−4826.5	−0.0030	TrES	2455365.8897	−206.5	−0.0009	QES
2453182.8991	−4970.5	−0.0028	TrES	2454230.6345	−2684	−0.0012	SWASP	2455366.8055	−204.5	−0.0015	QES
2453183.8157	−4968.5	−0.0027	TrES	2454232.6947	−2679.5	−0.0030	SWASP	2455367.7219	−202.5	−0.0016	QES
2453184.7320	−4966.5	−0.0028	TrES	2454233.6126	−2677.5	−0.0016	SWASP	2455370.7014	−196	−0.0005	QES
2453184.9616	−4966	−0.0024	TrES	2454235.6749	−2673	−0.0013	SWASP	2455382.8421	−169.5	−0.0028	QES
2453185.8783	−4964	−0.0021	TrES	2454236.5903	−2671	−0.0024	SWASP	2455383.7616	−167.5	0.0002	QES
2453187.9406	−4959.5	−0.0018	TrES	2454247.5886	−2647	−0.0015	SWASP	2455388.8006	−156.5	−0.0013	QES
2453189.7731	−4955.5	−0.0023	TrES	2454249.6512	−2642.5	−0.0009	SWASP	2455391.7788	−150	−0.0016	QES
2453190.9187	−4953	−0.0022	TrES	2454250.5675	−2640.5	−0.0010	SWASP	2455394.7563	−143.5	−0.0025	QES
2453191.8352	−4951	−0.0021	TrES	2454261.5641	−2616.5	−0.0019	SWASP	2455397.7352	−137	−0.0021	QES
2453192.7520	−4949	−0.0018	TrES	2454263.6261	−2612	−0.0018	SWASP	2455398.8821	−134.5	−0.0007	QES
2453192.9800	−4948.5	−0.0029	TrES	2454263.6271	−2612	−0.0008	SWASP	2455399.7972	−132.5	−0.0021	QES
2453194.8130	−4944.5	−0.0029	TrES	2454264.5430	−2610	−0.0014	SWASP	2455405.7542	−119.5	−0.0020	QES
2453196.8757	−4940	−0.0022	TrES	2454264.5434	−2610	−0.0010	SWASP	2455410.7945	−108.5	−0.0022	QES
2453198.7076	−4936	−0.0031	TrES	2454265.6872	−2607.5	−0.0027	SWASP	2455411.7117	−106.5	−0.0015	QES
2453198.9380	−4935.5	−0.0018	TrES	2454265.6889	−2607.5	−0.0011	SWASP	2455411.9396	−106	−0.0027	QES
2453204.8938	−4922.5	−0.0030	TrES	2454266.6043	−2605.5	−0.0021	SWASP	2455412.8570	−104	−0.0017	QES
2453205.8105	−4920.5	−0.0027	TrES	2454266.6056	−2605.5	−0.0009	SWASP	2455413.7728	−102	−0.0024	QES
2453206.7266	−4918.5	−0.0031	TrES	2454267.5207	−2603.5	−0.0022	SWASP	2455415.8351	−97.5	−0.0022	QES
2453206.9567	−4918	−0.0021	TrES	2454268.6672	−2601	−0.0013	SWASP	2455416.7517	−95.5	−0.0020	QES
2453207.8724	−4916	−0.0029	TrES	2454269.5819	−2599	−0.0030	SWASP	2455419.7306	−89	−0.0016	QES
2453208.7894	−4914	−0.0023	TrES	2454270.4984	−2597	−0.0030	SWASP	2455420.8754	−86.5	−0.0023	QES
2453209.7056	−4912	−0.0026	TrES	2454271.6449	−2594.5	−0.0020	SWASP	2455425.6865	−76	−0.0026	QES
2453209.9352	−4911.5	−0.0021	TrES	2454272.5624	−2592.5	−0.0010	SWASP	2455428.6649	−69.5	−0.0027	QES
2453210.8513	−4909.5	−0.0024	TrES	2454273.4787	−2590.5	−0.0012	SWASP	2455431.8731	−62.5	−0.0020	QES
2453211.7685	−4907.5	−0.0017	TrES	2454274.6226	−2588	−0.0028	SWASP	2455435.7683	−54	−0.0018	QES
2453212.6845	−4905.5	−0.0021	TrES	2454274.6230	−2588	−0.0024	SWASP	2455437.8303	−49.5	−0.0018	QES
2453213.8306	−4903	−0.0016	TrES	2454275.5409	−2586	−0.0010	SWASP	2455441.7257	−41	−0.0013	QES
2453214.7460	−4901	−0.0027	TrES	2454276.6848	−2583.5	−0.0026	SWASP	2455442.6411	−39	−0.0024	QES
2453214.9759	−4900.5	−0.0018	TrES	2454277.6019	−2581.5	−0.0019	SWASP	2455443.7876	−36.5	−0.0015	QES
2453215.8923	−4898.5	−0.0019	TrES	2454278.5190	−2579.5	−0.0013	SWASP	2455444.7040	−34.5	−0.0014	QES
2453216.8078	−4896.5	−0.0029	TrES	2454280.5802	−2575	−0.0021	SWASP	2455445.8491	−32	−0.0020	QES
2453217.7243	−4894.5	−0.0028	TrES	2454282.6422	−2570.5	−0.0021	SWASP	2455446.7651	−30	−0.0024	QES
2453217.9537	−4894	−0.0025	TrES	2454283.5586	−2568.5	−0.0022	SWASP	2455447.6818	−28	−0.0022	QES
2453218.8699	−4892	−0.0028	TrES	2454285.6211	−2564	−0.0017	SWASP	2455449.7439	−23.5	−0.0021	QES
2453219.7872	−4890	−0.0019	TrES	2454285.6212	−2564	−0.0016	SWASP	2455450.6605	−21.5	−0.0020	QES

Table 7
(Continued)

Min.	Epoch	$O-C$	Reference	Min.	Epoch	$O-C$	Reference	Min.	Epoch	$O-C$	Reference
2453220.7037	−4888	−0.0018	TrES	2454286.5370	−2562	−0.0023	SWASP	2455451.8060	−19	−0.0020	QES
2453220.9323	−4887.5	−0.0024	TrES	2454286.5378	−2562	−0.0014	SWASP	2455452.7229	−17	−0.0015	QES
2453221.8493	−4885.5	−0.0019	TrES	2454287.4536	−2560	−0.0021	SWASP	2455455.7016	−10.5	−0.0013	QES
2453222.7654	−4883.5	−0.0022	TrES	2454287.6820	−2559.5	−0.0028	SWASP	2455457.7636	−6	−0.0013	QES
2453222.9937	−4883	−0.0030	TrES	2454288.5980	−2557.5	−0.0032	SWASP	2455461.6581	2.5	−0.0017	QES
2453223.6811	−4881.5	−0.0030	TrES	2454288.5988	−2557.5	−0.0025	SWASP	2455463.7195	7	−0.0024	QES
2453223.9100	−4881	−0.0031	TrES	2454289.5161	−2555.5	−0.0016	SWASP	2455465.7827	11.5	−0.0011	QES
2453224.8275	−4879	−0.0021	TrES	2454289.5164	−2555.5	−0.0013	SWASP	2455466.6988	13.5	−0.0015	QES
2453226.8895	−4874.5	−0.0022	TrES	2454290.6610	−2553	−0.0023	SWASP	2455516.6455	122.5	−0.0015	QES
2453227.8057	−4872.5	−0.0023	TrES	2454291.5770	−2551	−0.0028	SWASP	2455666.9451	450.5	0.0001	QES
2453228.7215	−4870.5	−0.0031	TrES	2454291.5782	−2551	−0.0016	SWASP	2455669.9236	457	0.0001	QES
2453228.9502	−4870	−0.0034	TrES	2454292.4955	−2549	−0.0007	SWASP	2455697.8757	518	0.0004	QES
2453229.8682	−4868	−0.0018	TrES	2454293.6391	−2546.5	−0.0027	SWASP	2455702.9157	529	−0.0002	QES
2453230.7843	−4866	−0.0023	TrES	2454293.6401	−2546.5	−0.0017	SWASP	2455719.8703	566	0.0001	QES
2453234.6791	−4857.5	−0.0023	TrES	2454294.5555	−2544.5	−0.0027	SWASP	2455723.7656	574.5	0.0005	QES
2453234.9083	−4857	−0.0023	TrES	2454294.5561	−2544.5	−0.0021	SWASP	2455724.6814	576.5	−0.0001	QES
2453236.7417	−4853	−0.0018	TrES	2454295.4722	−2542.5	−0.0025	SWASP	2455724.9113	577	0.0006	QES
2453237.6575	−4851	−0.0025	TrES	2454295.4728	−2542.5	−0.0018	SWASP	2455725.8276	579	0.0005	QES
2453237.8863	−4850.5	−0.0028	TrES	2454296.6188	−2540	−0.0014	SWASP	2455727.8890	583.5	−0.0001	QES
2453239.7188	−4846.5	−0.0031	TrES	2454637.5390	−1796	−0.0014	SWASP	2455730.8681	590	0.0005	QES

Min.	Epoch	$O-C$	Reference	Min.	Epoch	$O-C$	Reference	Min.	Epoch	$O-C$	Reference
2455731.7847	592	0.0006	QES	2458 689.8658	7047.5	0.0038	TESS	2458698.5724	7066.5	0.0041	TESS
2455732.7002	594	−0.0003	QES	2458 689.8658	7047.5	0.0038	TESS	2458698.5724	7066.5	0.0041	TESS
2455733.8467	596.5	0.0006	QES	2458690.0948	7048	0.0037	TESS	2458698.8009	7067	0.0035	TESS
2455734.7625	598.5	−0.0001	QES	2458690.0948	7048	0.0037	TESS	2458698.8011	7067	0.0037	TESS
2455735.6796	600.5	0.0006	QES	2458690.3238	7048.5	0.0035	TESS	2458699.0307	7067.5	0.0042	TESS
2455735.9089	601	0.0009	QES	2458690.3238	7048.5	0.0035	TESS	2458699.0307	7067.5	0.0042	TESS
2455736.8251	603	0.0006	QES	2458690.5532	7049	0.0039	TESS	2458699.2600	7068	0.0044	TESS
2455737.7413	605	0.0003	QES	2458690.5532	7049	0.0039	TESS	2458699.2601	7068	0.0044	TESS
2455738.8873	607.5	0.0008	QES	2458690.7820	7049.5	0.0036	TESS	2458699.4885	7068.5	0.0037	TESS
2455739.8035	609.5	0.0005	QES	2458690.7821	7049.5	0.0037	TESS	2458699.4885	7068.5	0.0037	TESS
2455741.8653	614	0.0002	QES	2458691.0111	7050	0.0036	TESS	2458699.7182	7069	0.0044	TESS
2455742.7823	616	0.0008	QES	2458691.0111	7050	0.0036	TESS	2458699.7182	7069	0.0044	TESS
2458683.4508	7033.5	0.0040	TESS	2458691.2408	7050.5	0.0041	TESS	2458699.9473	7069.5	0.0043	TESS
2458683.4508	7033.5	0.0040	TESS	2458691.2408	7050.5	0.0041	TESS	2458699.9473	7069.5	0.0043	TESS
2458683.6796	7034	0.0037	TESS	2458691.4703	7051	0.0045	TESS	2458700.1763	7070	0.0042	TESS
2458683.6796	7034	0.0037	TESS	2458691.4704	7051	0.0046	TESS	2458700.1763	7070	0.0042	TESS
2458683.9095	7034.5	0.0044	TESS	2458691.6987	7051.5	0.0038	TESS	2458700.4051	7070.5	0.0040	TESS
2458683.9095	7034.5	0.0044	TESS	2458691.6987	7051.5	0.0038	TESS	2458700.4051	7070.5	0.0040	TESS
2458684.1384	7035	0.0042	TESS	2458691.9283	7052	0.0043	TESS	2458700.6347	7071	0.0044	TESS
2458684.1384	7035	0.0042	TESS	2458691.9283	7052	0.0043	TESS	2458700.6348	7071	0.0045	TESS
2458684.3677	7035.5	0.0045	TESS	2458692.1565	7052.5	0.0034	TESS	2458700.8635	7071.5	0.0041	TESS
2458684.3677	7035.5	0.0045	TESS	2458692.1567	7052.5	0.0036	TESS	2458700.8635	7071.5	0.0041	TESS
2458684.5959	7036	0.0035	TESS	2458692.3860	7053	0.0037	TESS	2458701.0922	7072	0.0037	TESS
2458684.5960	7036	0.0036	TESS	2458692.3861	7053	0.0038	TESS	2458701.0922	7072	0.0037	TESS
2458684.8257	7036.5	0.0042	TESS	2458692.6151	7053.5	0.0037	TESS	2458701.3213	7072.5	0.0037	TESS

Table 7
(Continued)

Min.	Epoch	$O-C$	Reference	Min.	Epoch	$O-C$	Reference	Min.	Epoch	$O-C$	Reference
2458684.8257	7036.5	0.0042	TESS	2458692.6151	7053.5	0.0037	TESS	2458701.3214	7072.5	0.0038	TESS
2458685.0542	7037	0.0036	TESS	2458692.8444	7054	0.0040	TESS	2458701.5512	7073	0.0045	TESS
2458685.0544	7037	0.0038	TESS	2458692.8444	7054	0.0040	TESS	2458701.5515	7073	0.0047	TESS
2458685.2837	7037.5	0.0040	TESS	2458693.0732	7054.5	0.0036	TESS	2458701.7794	7073.5	0.0035	TESS
2458685.2837	7037.5	0.0040	TESS	2458693.0732	7054.5	0.0036	TESS	2458701.7796	7073.5	0.0037	TESS
2458685.5124	7038	0.0036	TESS	2458693.3027	7055	0.0040	TESS	2458702.0085	7074	0.0035	TESS
2458685.5126	7038	0.0038	TESS	2458693.3027	7055	0.0040	TESS	2458702.0088	7074	0.0038	TESS
2458685.7417	7038.5	0.0037	TESS	2458693.5315	7055.5	0.0037	TESS	2458702.2382	7074.5	0.0041	TESS
2458685.7417	7038.5	0.0037	TESS	2458693.5317	7055.5	0.0039	TESS	2458702.2382	7074.5	0.0041	TESS
2458685.9706	7039	0.0036	TESS	2458693.7604	7056	0.0035	TESS	2458702.4673	7075	0.0041	TESS
2458685.9709	7039	0.0039	TESS	2458693.7606	7056	0.0037	TESS	2458702.4673	7075	0.0041	TESS
2458686.2002	7039.5	0.0040	TESS	2458693.9901	7056.5	0.0041	TESS	2458702.6968	7075.5	0.0044	TESS
2458686.2002	7039.5	0.0040	TESS	2458693.9901	7056.5	0.0041	TESS	2458702.6971	7075.5	0.0047	TESS
2458686.4293	7040	0.0040	TESS	2458694.2194	7057	0.0043	TESS	2458702.9252	7076	0.0038	TESS
2458686.4293	7040	0.0040	TESS	2458694.2194	7057	0.0043	TESS	2458702.9252	7076	0.0038	TESS
2458686.6582	7040.5	0.0037	TESS	2458694.4480	7057.5	0.0038	TESS	2458703.1549	7076.5	0.0044	TESS
2458686.6582	7040.5	0.0037	TESS	2458694.4480	7057.5	0.0038	TESS	2458703.1550	7076.5	0.0045	TESS
2458686.8871	7041	0.0036	TESS	2458694.6777	7058	0.0044	TESS	2458703.3832	7077	0.0035	TESS
2458686.8871	7041	0.0036	TESS	2458694.6777	7058	0.0044	TESS	2458703.3833	7077	0.0037	TESS
2458687.1162	7041.5	0.0036	TESS	2458694.9068	7058.5	0.0044	TESS	2458703.6131	7077.5	0.0044	TESS
2458687.1165	7041.5	0.0039	TESS	2458694.9069	7058.5	0.0045	TESS	2458703.6132	7077.5	0.0044	TESS
2458687.3453	7042	0.0036	TESS	2458695.1356	7059	0.0040	TESS	2458703.8416	7078	0.0037	TESS
2458687.3453	7042	0.0036	TESS	2458695.1356	7059	0.0040	TESS	2458703.8416	7078	0.0037	TESS
2458687.5746	7042.5	0.0038	TESS	2458695.3649	7059.5	0.0042	TESS	2458704.0714	7078.5	0.0044	TESS
2458687.5746	7042.5	0.0038	TESS	2458695.3651	7059.5	0.0044	TESS	2458704.0715	7078.5	0.0045	TESS
2458687.8043	7043	0.0043	TESS	2458695.5934	7060	0.0035	TESS	2458704.3001	7079	0.0040	TESS
2458687.8043	7043	0.0043	TESS	2458695.5934	7060	0.0035	TESS	2458704.3001	7079	0.0040	TESS
2458688.0330	7043.5	0.0039	TESS	2458695.8233	7060.5	0.0044	TESS	2458704.5293	7079.5	0.0041	TESS
2458688.0330	7043.5	0.0039	TESS	2458695.8234	7060.5	0.0045	TESS	2458704.5293	7079.5	0.0041	TESS
2458688.2621	7044	0.0039	TESS	2458696.0523	7061	0.0042	TESS	2458704.7587	7080	0.0044	TESS
2458688.2621	7044	0.0039	TESS	2458696.0523	7061	0.0042	TESS	2458704.7588	7080	0.0045	TESS
2458688.4917	7044.5	0.0044	TESS	2458696.2807	7061.5	0.0035	TESS	2458704.9877	7080.5	0.0043	TESS
2458688.4918	7044.5	0.0045	TESS	2458696.2809	7061.5	0.0037	TESS	2458704.9877	7080.5	0.0043	TESS
2458688.7207	7045	0.0043	TESS	2458697.4269	7064	0.0042	TESS	2458705.2167	7081	0.0042	TESS
2458688.7207	7045	0.0043	TESS	2458697.4269	7064	0.0042	TESS	2458705.2167	7081	0.0042	TESS
2458688.9492	7045.5	0.0037	TESS	2458697.6563	7064.5	0.0045	TESS	2458705.4460	7081.5	0.0043	TESS
2458688.9492	7045.5	0.0037	TESS	2458697.6563	7064.5	0.0045	TESS	2458705.4460	7081.5	0.0043	TESS
2458689.1790	7046	0.0043	TESS	2458697.8854	7065	0.0045	TESS	2458705.6749	7082	0.0041	TESS
2458689.1790	7046	0.0043	TESS	2458697.8854	7065	0.0045	TESS	2458705.6749	7082	0.0041	TESS
2458689.4077	7046.5	0.0040	TESS	2458698.1145	7065.5	0.0044	TESS	2458705.9041	7082.5	0.0042	TESS
2458689.4077	7046.5	0.0040	TESS	2458698.1145	7065.5	0.0044	TESS	2458705.9041	7082.5	0.0042	TESS
2458689.6366	7047	0.0037	TESS	2458698.3436	7066	0.0044	TESS	2458706.1331	7083	0.0041	TESS
2458689.6366	7047	0.0037	TESS	2458698.3437	7066	0.0045	TESS	2458706.1331	7083	0.0041	TESS
Min.	Epoch	$O-C$	Reference	Min.	Epoch	$O-C$	Reference	Min.	Epoch	$O-C$	Reference
2458706.3625	7083.5	0.0044	TESS	2458719.4224	7112	0.0048	TESS	2458736.3769	7149	0.0050	TESS
2458706.3626	7083.5	0.0045	TESS	2458719.6521	7112.5	0.0055	TESS	2458736.6065	7149.5	0.0054	TESS
2458706.5913	7084	0.0041	TESS	2458719.8811	7113	0.0053	TESS	2458736.8352	7150	0.0051	TESS

Table 7
(Continued)

Min.	Epoch	$O-C$	Reference	Min.	Epoch	$O-C$	Reference	Min.	Epoch	$O-C$	Reference
2458706.5913	7084	0.0041	TESS	2458720.1096	7113.5	0.0047	TESS	2458737.0646	7150.5	0.0054	TESS
2458706.8206	7084.5	0.0043	TESS	2458720.3389	7114	0.0049	TESS	2458737.2932	7151	0.0048	TESS
2458706.8206	7084.5	0.0043	TESS	2458720.5686	7114.5	0.0055	TESS	2458738.8994	7154.5	0.0072	TESS
2458707.0498	7085	0.0043	TESS	2458720.7970	7115	0.0047	TESS	2458739.1287	7155	0.0074	TESS
2458707.0499	7085	0.0045	TESS	2458721.0261	7115.5	0.0047	TESS	2458739.3573	7155.5	0.0069	TESS
2458707.2783	7085.5	0.0037	TESS	2458721.2554	7116	0.0049	TESS	2458739.5866	7156	0.0070	TESS
2458707.2783	7085.5	0.0037	TESS	2458721.4849	7116.5	0.0053	TESS	2458739.8154	7156.5	0.0068	TESS
2458707.5074	7086	0.0037	TESS	2458721.7138	7117	0.0051	TESS	2458740.0453	7157	0.0076	TESS
2458707.5074	7086	0.0037	TESS	2458721.9431	7117.5	0.0053	TESS	2458740.2736	7157.5	0.0068	TESS
2458707.7371	7086.5	0.0043	TESS	2458722.1723	7118	0.0054	TESS	2458740.5035	7158	0.0075	TESS
2458707.7372	7086.5	0.0044	TESS	2458722.4010	7118.5	0.0050	TESS	2458740.7320	7158.5	0.0069	TESS
2458707.9655	7087	0.0035	TESS	2458722.6299	7119	0.0047	TESS	2458740.9612	7159	0.0070	TESS
2458707.9656	7087	0.0036	TESS	2458722.8588	7119.5	0.0046	TESS	2458741.1901	7159.5	0.0068	TESS
2458708.1946	7087.5	0.0035	TESS	2458723.0880	7120	0.0046	TESS	2458741.4198	7160	0.0073	TESS
2458708.1946	7087.5	0.0036	TESS	2458723.3172	7120.5	0.0047	TESS	2458741.6487	7160.5	0.0072	TESS
2458708.4237	7088	0.0035	TESS	2458723.5462	7121	0.0046	TESS	2458741.8776	7161	0.0070	TESS
2458708.4237	7088	0.0036	TESS	2458723.7760	7121.5	0.0053	TESS	2458742.1067	7161.5	0.0070	TESS
2458708.6533	7088.5	0.0040	TESS	2458725.3794	7125	0.0049	TESS	2458742.3362	7162	0.0074	TESS
2458708.6533	7088.5	0.0040	TESS	2458725.6088	7125.5	0.0052	TESS	2458742.5652	7162.5	0.0072	TESS
2458708.8827	7089	0.0044	TESS	2458725.8383	7126	0.0056	TESS	2458742.7947	7163	0.0076	TESS
2458708.8828	7089	0.0045	TESS	2458726.0665	7126.5	0.0047	TESS	2458743.0239	7163.5	0.0077	TESS
2458709.1119	7089.5	0.0044	TESS	2458726.2959	7127	0.0049	TESS	2458743.2530	7164	0.0077	TESS
2458709.1119	7089.5	0.0044	TESS	2458726.5250	7127.5	0.0049	TESS	2458743.4819	7164.5	0.0075	TESS
2458709.3411	7090	0.0045	TESS	2458726.7538	7128	0.0046	TESS	2458743.7112	7165	0.0077	TESS
2458709.3411	7090	0.0045	TESS	2458726.9837	7128.5	0.0054	TESS	2458743.9402	7165.5	0.0075	TESS
2458709.5701	7090.5	0.0044	TESS	2458727.2125	7129	0.0051	TESS	2458744.1693	7166	0.0076	TESS
2458709.5701	7090.5	0.0044	TESS	2458727.4418	7129.5	0.0053	TESS	2458744.3979	7166.5	0.0070	TESS
2458709.7991	7091	0.0043	TESS	2458727.6711	7130	0.0054	TESS	2458744.6268	7167	0.0068	TESS
2458709.7992	7091	0.0044	TESS	2458727.9001	7130.5	0.0054	TESS	2458744.8565	7167.5	0.0074	TESS
2458710.0277	7091.5	0.0038	TESS	2458728.1291	7131	0.0052	TESS	2458745.0858	7168	0.0076	TESS
2458710.0277	7091.5	0.0038	TESS	2458728.3584	7131.5	0.0054	TESS	2458745.3147	7168.5	0.0074	TESS
2458711.6323	7095	0.0046	TESS	2458728.5872	7132	0.0051	TESS	2458745.5439	7169	0.0074	TESS
2458711.8623	7095.5	0.0055	TESS	2458728.8166	7132.5	0.0054	TESS	2458745.7730	7169.5	0.0075	TESS
2458712.0905	7096	0.0045	TESS	2458729.0454	7133	0.0051	TESS	2458746.0015	7170	0.0069	TESS
2458712.3197	7096.5	0.0047	TESS	2458729.2744	7133.5	0.0050	TESS	2458746.2311	7170.5	0.0074	TESS
2458712.5488	7097	0.0046	TESS	2458729.5039	7134	0.0053	TESS	2458746.4597	7171	0.0068	TESS
2458712.7787	7097.5	0.0054	TESS	2458729.7331	7134.5	0.0054	TESS	2458746.6895	7171.5	0.0075	TESS
2458713.0070	7098	0.0046	TESS	2458729.9620	7135	0.0052	TESS	2458746.9180	7172	0.0069	TESS
2458713.2370	7098.5	0.0055	TESS	2458730.1914	7135.5	0.0055	TESS	2458747.1473	7172.5	0.0071	TESS
2458713.4652	7099	0.0046	TESS	2458730.4202	7136	0.0052	TESS	2458747.3770	7173	0.0077	TESS
2458713.6945	7099.5	0.0048	TESS	2458730.6492	7136.5	0.0051	TESS	2458747.6060	7173.5	0.0076	TESS
2458713.9236	7100	0.0047	TESS	2458730.8783	7137	0.0050	TESS	2458747.8351	7174	0.0075	TESS
2458714.1527	7100.5	0.0048	TESS	2458731.1071	7137.5	0.0048	TESS	2458748.0644	7174.5	0.0077	TESS
2458714.3821	7101	0.0050	TESS	2458731.3368	7138	0.0054	TESS	2458748.2928	7175	0.0070	TESS
2458714.6116	7101.5	0.0054	TESS	2458731.5656	7138.5	0.0050	TESS	2458748.5225	7175.5	0.0076	TESS
2458714.8407	7102	0.0054	TESS	2458731.7949	7139	0.0053	TESS	2458748.7514	7176	0.0073	TESS
2458715.0695	7102.5	0.0051	TESS	2458732.0238	7139.5	0.0050	TESS	2458748.9803	7176.5	0.0072	TESS
2458715.2983	7103	0.0047	TESS	2458732.2529	7140	0.0050	TESS	2458749.2096	7177	0.0074	TESS

Table 7
(Continued)

Min.	Epoch	$O-C$	Reference	Min.	Epoch	$O-C$	Reference	Min.	Epoch	$O-C$	Reference
2458715.5276	7103.5	0.0050	TESS	2458732.4817	7140.5	0.0047	TESS	2458749.4387	7177.5	0.0073	TESS
2458715.7564	7104	0.0046	TESS	2458732.7115	7141	0.0054	TESS	2458749.6681	7178	0.0077	TESS
2458715.9856	7104.5	0.0047	TESS	2458732.9399	7141.5	0.0046	TESS	2458749.8966	7178.5	0.0070	TESS
2458716.2145	7105	0.0045	TESS	2458733.1698	7142	0.0054	TESS	2458750.1254	7179	0.0067	TESS
2458716.4443	7105.5	0.0052	TESS	2458733.3984	7142.5	0.0049	TESS	2458751.9585	7183	0.0069	TESS
2458716.6728	7106	0.0046	TESS	2458733.6279	7143	0.0054	TESS	2458752.1875	7183.5	0.0067	TESS
2458716.9024	7106.5	0.0051	TESS	2458733.8570	7143.5	0.0053	TESS	2458752.4167	7184	0.0068	TESS
2458717.1310	7107	0.0046	TESS	2458734.0862	7144	0.0054	TESS	2458752.6466	7184.5	0.0077	TESS
2458717.3605	7107.5	0.0049	TESS	2458734.3145	7144.5	0.0046	TESS	2458752.8748	7185	0.0067	TESS
2458717.5900	7108	0.0053	TESS	2458734.5442	7145	0.0052	TESS	2458753.1043	7185.5	0.0071	TESS
2458717.8184	7108.5	0.0046	TESS	2458734.7736	7145.5	0.0054	TESS	2458753.3334	7186	0.0071	TESS
2458718.0474	7109	0.0046	TESS	2458735.0025	7146	0.0052	TESS	2458753.5630	7186.5	0.0076	TESS
2458718.2766	7109.5	0.0046	TESS	2458735.2314	7146.5	0.0051	TESS	2458753.7913	7187	0.0068	TESS
2458718.5062	7110	0.0051	TESS	2458735.4605	7147	0.0050	TESS	2458754.0208	7187.5	0.0072	TESS
2458718.7353	7110.5	0.0051	TESS	2458735.6900	7147.5	0.0054	TESS	2458754.2495	7188	0.0068	TESS
2458718.9639	7111	0.0046	TESS	2458735.9188	7148	0.0051	TESS	2458754.4795	7188.5	0.0077	TESS
2458719.1934	7111.5	0.0050	TESS	2458736.1480	7148.5	0.0052	TESS	2458754.7077	7189	0.0067	TESS
Min.	Epoch	$O-C$	Reference	Min.	Epoch	$O-C$	Reference	Min.	Epoch	$O-C$	Reference
2458754.9374	7189.5	0.0073	TESS	2459423.4912	8648.5	0.0094	TESS	2459431.5101	8666	0.0094	TESS
2458755.1660	7190	0.0068	TESS	2459423.7195	8649	0.0085	TESS	2459431.7388	8666.5	0.0090	TESS
2458755.3955	7190.5	0.0071	TESS	2459423.7197	8649	0.0087	TESS	2459431.7388	8666.5	0.0090	TESS
2458755.6245	7191	0.0071	TESS	2459423.9488	8649.5	0.0087	TESS	2459431.9679	8667	0.0089	TESS
2458755.8542	7191.5	0.0077	TESS	2459423.9488	8649.5	0.0087	TESS	2459431.9679	8667	0.0089	TESS
2458756.0824	7192	0.0068	TESS	2459424.1777	8650	0.0086	TESS	2459432.1967	8667.5	0.0086	TESS
2458756.3119	7192.5	0.0071	TESS	2459424.1778	8650	0.0087	TESS	2459432.1967	8667.5	0.0086	TESS
2458756.5407	7193	0.0069	TESS	2459424.4073	8650.5	0.0090	TESS	2459432.4263	8668	0.0091	TESS
2458756.7700	7193.5	0.0071	TESS	2459424.4073	8650.5	0.0090	TESS	2459432.4263	8668	0.0091	TESS
2458756.9989	7194	0.0068	TESS	2459424.6361	8651	0.0087	TESS	2459433.8013	8671	0.0094	TESS
2458757.2283	7194.5	0.0071	TESS	2459424.6361	8651	0.0087	TESS	2459433.8013	8671	0.0094	TESS
2458757.4571	7195	0.0067	TESS	2459424.8653	8651.5	0.0088	TESS	2459434.0298	8671.5	0.0087	TESS
2458757.6871	7195.5	0.0076	TESS	2459424.8653	8651.5	0.0088	TESS	2459434.0298	8671.5	0.0087	TESS
2458757.9158	7196	0.0073	TESS	2459425.0943	8652	0.0087	TESS	2459434.2590	8672	0.0089	TESS
2458758.1453	7196.5	0.0076	TESS	2459425.0943	8652	0.0087	TESS	2459434.2590	8672	0.0089	TESS
2458758.3743	7197	0.0076	TESS	2459425.3231	8652.5	0.0084	TESS	2459434.4878	8672.5	0.0085	TESS
2458758.6031	7197.5	0.0072	TESS	2459425.3233	8652.5	0.0086	TESS	2459434.4881	8672.5	0.0088	TESS
2458758.8326	7198	0.0076	TESS	2459425.5525	8653	0.0087	TESS	2459434.7174	8673	0.0091	TESS
2458759.0608	7198.5	0.0067	TESS	2459425.5529	8653	0.0091	TESS	2459434.7174	8673	0.0091	TESS
2458759.2909	7199	0.0076	TESS	2459425.7815	8653.5	0.0085	TESS	2459434.9468	8673.5	0.0093	TESS
2458759.5200	7199.5	0.0077	TESS	2459425.7816	8653.5	0.0086	TESS	2459434.9468	8673.5	0.0093	TESS
2458759.7488	7200	0.0074	TESS	2459426.0114	8654	0.0093	TESS	2459435.1759	8674	0.0094	TESS
2458759.9776	7200.5	0.0070	TESS	2459426.0114	8654	0.0093	TESS	2459435.1760	8674	0.0094	TESS
2458760.2065	7201	0.0068	TESS	2459426.4690	8655	0.0087	TESS	2459435.4047	8674.5	0.0091	TESS
2458760.4357	7201.5	0.0069	TESS	2459426.4690	8655	0.0087	TESS	2459435.4047	8674.5	0.0091	TESS
2458760.6646	7202	0.0067	TESS	2459426.6982	8655.5	0.0088	TESS	2459435.6337	8675	0.0089	TESS
2458760.8945	7202.5	0.0075	TESS	2459426.6982	8655.5	0.0088	TESS	2459435.6337	8675	0.0089	TESS
2458761.1229	7203	0.0067	TESS	2459426.9272	8656	0.0087	TESS	2459435.8631	8675.5	0.0092	TESS
2458761.3529	7203.5	0.0077	TESS	2459426.9272	8656	0.0087	TESS	2459435.8633	8675.5	0.0094	TESS

Table 7
(Continued)

Min.	Epoch	$O-C$	Reference	Min.	Epoch	$O-C$	Reference	Min.	Epoch	$O-C$	Reference
2458761.5812	7204	0.0069	TESS	2459427.1566	8656.5	0.0090	TESS	2459436.0923	8676	0.0093	TESS
2458761.8104	7204.5	0.0070	TESS	2459427.1566	8656.5	0.0090	TESS	2459436.0924	8676	0.0094	TESS
2458762.0394	7205	0.0068	TESS	2459427.3856	8657	0.0089	TESS	2459436.3207	8676.5	0.0086	TESS
2458762.2692	7205.5	0.0075	TESS	2459427.3856	8657	0.0089	TESS	2459436.3208	8676.5	0.0087	TESS
2458762.4977	7206	0.0069	TESS	2459427.6148	8657.5	0.0089	TESS	2459436.5507	8677	0.0094	TESS
2458762.7275	7206.5	0.0076	TESS	2459427.6148	8657.5	0.0089	TESS	2459436.5507	8677	0.0095	TESS
2458762.9559	7207	0.0068	TESS	2459427.8435	8658	0.0085	TESS	2459436.7794	8677.5	0.0091	TESS
2458763.1857	7207.5	0.0075	TESS	2459427.8437	8658	0.0087	TESS	2459436.7794	8677.5	0.0091	TESS
2459420.0544	8641	0.0093	TESS	2459428.0725	8658.5	0.0084	TESS	2459437.0084	8678	0.0089	TESS
2459420.0544	8641	0.0093	TESS	2459428.0727	8658.5	0.0086	TESS	2459437.0084	8678	0.0089	TESS
2459420.2831	8641.5	0.0089	TESS	2459428.3019	8659	0.0087	TESS	2459437.2379	8678.5	0.0093	TESS
2459420.2831	8641.5	0.0089	TESS	2459428.3019	8659	0.0087	TESS	2459437.2380	8678.5	0.0094	TESS
2459420.5125	8642	0.0092	TESS	2459428.5308	8659.5	0.0085	TESS	2459437.4667	8679	0.0090	TESS
2459420.5125	8642	0.0092	TESS	2459428.5310	8659.5	0.0087	TESS	2459437.4667	8679	0.0090	TESS
2459420.7414	8642.5	0.0089	TESS	2459428.7599	8660	0.0085	TESS	2459437.6958	8679.5	0.0089	TESS
2459420.7414	8642.5	0.0089	TESS	2459428.7602	8660	0.0088	TESS	2459437.6958	8679.5	0.0089	TESS
2459420.9708	8643	0.0093	TESS	2459428.9891	8660.5	0.0086	TESS	2459437.9251	8680	0.0091	TESS
2459420.9708	8643	0.0093	TESS	2459428.9891	8660.5	0.0086	TESS	2459437.9251	8680	0.0091	TESS
2459421.1994	8643.5	0.0087	TESS	2459429.2184	8661	0.0087	TESS	2459438.1539	8680.5	0.0089	TESS
2459421.1994	8643.5	0.0087	TESS	2459429.2184	8661	0.0087	TESS	2459438.1539	8680.5	0.0089	TESS
2459421.4291	8644	0.0093	TESS	2459429.4479	8661.5	0.0091	TESS	2459438.3829	8681	0.0087	TESS
2459421.4291	8644	0.0093	TESS	2459429.4481	8661.5	0.0093	TESS	2459438.3829	8681	0.0087	TESS
2459421.6577	8644.5	0.0088	TESS	2459429.6768	8662	0.0089	TESS	2459438.6123	8681.5	0.0090	TESS
2459421.6577	8644.5	0.0088	TESS	2459429.6768	8662	0.0089	TESS	2459438.6123	8681.5	0.0090	TESS
2459421.8866	8645	0.0085	TESS	2459429.9056	8662.5	0.0087	TESS	2459438.8415	8682	0.0091	TESS
2459421.8869	8645	0.0088	TESS	2459429.9056	8662.5	0.0087	TESS	2459438.8415	8682	0.0091	TESS
2459422.1156	8645.5	0.0084	TESS	2459430.1346	8663	0.0085	TESS	2459439.0707	8682.5	0.0092	TESS
2459422.1161	8645.5	0.0089	TESS	2459430.1347	8663	0.0087	TESS	2459439.0707	8682.5	0.0092	TESS
2459422.3456	8646	0.0093	TESS	2459430.3637	8663.5	0.0085	TESS	2459439.2991	8683	0.0084	TESS
2459422.3456	8646	0.0093	TESS	2459430.3640	8663.5	0.0088	TESS	2459439.2994	8683	0.0087	TESS
2459422.5744	8646.5	0.0091	TESS	2459430.5929	8664	0.0085	TESS	2459439.5290	8683.5	0.0093	TESS
2459422.5744	8646.5	0.0091	TESS	2459430.5931	8664	0.0087	TESS	2459439.5291	8683.5	0.0094	TESS
2459422.8032	8647	0.0087	TESS	2459430.8222	8664.5	0.0088	TESS	2459439.7577	8684	0.0089	TESS
2459422.8032	8647	0.0087	TESS	2459430.8222	8664.5	0.0088	TESS	2459439.7577	8684	0.0089	TESS
2459423.0325	8647.5	0.0089	TESS	2459431.0516	8665	0.0091	TESS	2459439.9873	8684.5	0.0093	TESS
2459423.0325	8647.5	0.0089	TESS	2459431.0516	8665	0.0091	TESS	2459439.9874	8684.5	0.0094	TESS
2459423.2618	8648	0.0091	TESS	2459431.2802	8665.5	0.0085	TESS	2459440.2164	8685	0.0093	TESS
2459423.2618	8648	0.0091	TESS	2459431.2804	8665.5	0.0087	TESS	2459440.2164	8685	0.0094	TESS
2459423.4911	8648.5	0.0093	TESS	2459431.5100	8666	0.0093	TESS	2459440.4452	8685.5	0.0090	TESS
Min.	Epoch	$O-C$	Reference	Min.	Epoch	$O-C$	Reference	Min.	Epoch	$O-C$	Reference
2459440.4452	8685.5	0.0090	TESS	2459773.5766	9412.5	0.0101	TESS	2459790.3013	9449	0.0096	TESS
2459440.6740	8686	0.0087	TESS	2459773.8055	9413	0.0099	TESS	2459790.5311	9449.5	0.0103	TESS
2459440.6740	8686	0.0087	TESS	2459774.0348	9413.5	0.0101	TESS	2459790.7601	9450	0.0102	TESS
2459440.9038	8686.5	0.0094	TESS	2459774.2635	9414	0.0097	TESS	2459790.9893	9450.5	0.0102	TESS
2459440.9038	8686.5	0.0094	TESS	2459774.4930	9414.5	0.0101	TESS	2459791.2184	9451	0.0103	TESS
2459441.1327	8687	0.0092	TESS	2459774.7218	9415	0.0098	TESS	2459791.4477	9451.5	0.0104	TESS
2459441.1327	8687	0.0092	TESS	2459774.9516	9415.5	0.0105	TESS	2459791.6768	9452	0.0104	TESS

Table 7
(Continued)

Min.	Epoch	$O-C$	Reference	Min.	Epoch	$O-C$	Reference	Min.	Epoch	$O-C$	Reference
2459441.3619	8687.5	0.0093	TESS	2459775.1801	9416	0.0099	TESS	2459791.9051	9452.5	0.0096	TESS
2459441.3619	8687.5	0.0093	TESS	2459775.4093	9416.5	0.0099	TESS	2459792.1350	9453	0.0104	TESS
2459441.5905	8688	0.0087	TESS	2459775.6381	9417	0.0096	TESS	2459792.3638	9453.5	0.0101	TESS
2459441.5905	8688	0.0087	TESS	2459775.8680	9417.5	0.0104	TESS	2459792.5927	9454	0.0098	TESS
2459441.8198	8688.5	0.0089	TESS	2459776.0963	9418	0.0096	TESS	2459792.8224	9454.5	0.0105	TESS
2459441.8198	8688.5	0.0089	TESS	2459776.3261	9418.5	0.0103	TESS	2459793.0514	9455	0.0103	TESS
2459442.0490	8689	0.0090	TESS	2459776.5549	9419	0.0100	TESS	2459793.2804	9455.5	0.0102	TESS
2459442.0490	8689	0.0090	TESS	2459776.7844	9419.5	0.0104	TESS	2459793.5097	9456	0.0104	TESS
2459442.2780	8689.5	0.0089	TESS	2459777.0133	9420	0.0102	TESS	2459793.7387	9456.5	0.0103	TESS
2459442.2780	8689.5	0.0089	TESS	2459777.2427	9420.5	0.0104	TESS	2459793.9676	9457	0.0101	TESS
2459442.5066	8690	0.0084	TESS	2459777.4718	9421	0.0104	TESS	2459794.1971	9457.5	0.0105	TESS
2459442.5067	8690	0.0085	TESS	2459777.7004	9421.5	0.0099	TESS	2459794.4260	9458	0.0102	TESS
2459442.7357	8690.5	0.0084	TESS	2459777.9297	9422	0.0100	TESS	2459794.6552	9458.5	0.0103	TESS
2459442.7359	8690.5	0.0086	TESS	2459778.1584	9422.5	0.0096	TESS	2459794.8844	9459	0.0104	TESS
2459442.9656	8691	0.0092	TESS	2459778.3883	9423	0.0104	TESS	2459795.1135	9459.5	0.0104	TESS
2459442.9656	8691	0.0092	TESS	2459778.6166	9423.5	0.0096	TESS	2459795.3420	9460	0.0098	TESS
2459443.1941	8691.5	0.0086	TESS	2459778.8463	9424	0.0102	TESS	2459795.5717	9460.5	0.0103	TESS
2459443.1941	8691.5	0.0086	TESS	2459779.0755	9424.5	0.0103	TESS	2459795.8002	9461	0.0098	TESS
2459443.4240	8692	0.0094	TESS	2459779.3047	9425	0.0104	TESS	2459796.0300	9461.5	0.0104	TESS
2459443.4240	8692	0.0094	TESS	2459779.5333	9425.5	0.0099	TESS	2459797.1751	9464	0.0100	TESS
2459443.6527	8692.5	0.0089	TESS	2459779.7621	9426	0.0096	TESS	2459797.1751	9464	0.0100	TESS
2459443.6527	8692.5	0.0089	TESS	2459779.9916	9426.5	0.0100	TESS	2459797.4047	9464.5	0.0104	TESS
2459443.8822	8693	0.0093	TESS	2459780.2204	9427	0.0096	TESS	2459797.4048	9464.5	0.0105	TESS
2459443.8823	8693	0.0094	TESS	2459780.4495	9427.5	0.0096	TESS	2459797.6330	9465	0.0097	TESS
2459444.1113	8693.5	0.0093	TESS	2459780.6788	9428	0.0098	TESS	2459797.6330	9465	0.0097	TESS
2459444.1114	8693.5	0.0094	TESS	2459780.9077	9428.5	0.0096	TESS	2459797.8619	9465.5	0.0094	TESS
2459444.3405	8694	0.0094	TESS	2459781.1374	9429	0.0102	TESS	2459797.8622	9465.5	0.0097	TESS
2459444.3405	8694	0.0094	TESS	2459781.3659	9429.5	0.0096	TESS	2459798.0913	9466	0.0097	TESS
2459444.5696	8694.5	0.0093	TESS	2459781.5955	9430	0.0101	TESS	2459798.0913	9466	0.0097	TESS
2459444.5697	8694.5	0.0094	TESS	2459781.8248	9430.5	0.0103	TESS	2459798.3211	9466.5	0.0104	TESS
2459444.7986	8695	0.0093	TESS	2459782.0539	9431	0.0102	TESS	2459798.3213	9466.5	0.0106	TESS
2459444.7986	8695	0.0093	TESS	2459782.2828	9431.5	0.0100	TESS	2459798.5495	9467	0.0097	TESS
2459445.0277	8695.5	0.0093	TESS	2459783.6571	9434.5	0.0096	TESS	2459798.5495	9467	0.0097	TESS
2459445.0278	8695.5	0.0094	TESS	2459783.8864	9435	0.0099	TESS	2459798.7794	9467.5	0.0104	TESS
2459445.2565	8696	0.0090	TESS	2459784.1154	9435.5	0.0097	TESS	2459798.7794	9467.5	0.0104	TESS
2459445.2565	8696	0.0090	TESS	2459784.3446	9436	0.0098	TESS	2459799.0083	9468	0.0103	TESS
2459445.4854	8696.5	0.0088	TESS	2459784.5736	9436.5	0.0097	TESS	2459799.0083	9468	0.0103	TESS
2459445.4854	8696.5	0.0088	TESS	2459784.8031	9437	0.0100	TESS	2459799.2375	9468.5	0.0104	TESS
2459445.7149	8697	0.0091	TESS	2459785.0317	9437.5	0.0096	TESS	2459799.2375	9468.5	0.0104	TESS
2459445.7149	8697	0.0091	TESS	2459785.2614	9438	0.0102	TESS	2459799.4666	9469	0.0103	TESS
2459445.9439	8697.5	0.0090	TESS	2459785.4907	9438.5	0.0104	TESS	2459799.4668	9469	0.0105	TESS
2459445.9439	8697.5	0.0090	TESS	2459785.7191	9439	0.0096	TESS	2459799.6957	9469.5	0.0103	TESS
2459446.1726	8698	0.0086	TESS	2459785.9485	9439.5	0.0100	TESS	2459799.6957	9469.5	0.0103	TESS
2459446.1726	8698	0.0086	TESS	2459786.1774	9440	0.0097	TESS	2459799.9249	9470	0.0104	TESS
2459446.4025	8698.5	0.0093	TESS	2459786.4065	9440.5	0.0097	TESS	2459799.9249	9470	0.0104	TESS
2459446.4025	8698.5	0.0093	TESS	2459786.6356	9441	0.0097	TESS	2459800.1534	9470.5	0.0098	TESS
2459770.1398	9405	0.0100	TESS	2459786.8655	9441.5	0.0104	TESS	2459800.1534	9470.5	0.0098	TESS
2459770.3685	9405.5	0.0096	TESS	2459787.0940	9442	0.0098	TESS	2459800.3829	9471	0.0102	TESS

Table 7
(Continued)

Min.	Epoch	$O-C$	Reference	Min.	Epoch	$O-C$	Reference	Min.	Epoch	$O-C$	Reference
2459770.5976	9406	0.0096	TESS	2459787.3232	9442.5	0.0100	TESS	2459800.3829	9471	0.0102	TESS
2459770.8272	9406.5	0.0101	TESS	2459787.5526	9443	0.0103	TESS	2459800.6116	9471.5	0.0098	TESS
2459771.0562	9407	0.0099	TESS	2459787.7819	9443.5	0.0104	TESS	2459800.6116	9471.5	0.0098	TESS
2459771.2858	9407.5	0.0104	TESS	2459788.0106	9444	0.0100	TESS	2459800.8411	9472	0.0102	TESS
2459771.5144	9408	0.0100	TESS	2459788.2395	9444.5	0.0098	TESS	2459800.8411	9472	0.0102	TESS
2459771.7433	9408.5	0.0097	TESS	2459788.4691	9445	0.0102	TESS	2459801.0698	9472.5	0.0098	TESS
2459771.9722	9409	0.0095	TESS	2459788.6983	9445.5	0.0103	TESS	2459801.0698	9472.5	0.0098	TESS
2459772.2021	9409.5	0.0103	TESS	2459788.9270	9446	0.0100	TESS	2459801.2989	9473	0.0098	TESS
2459772.4310	9410	0.0101	TESS	2459789.1564	9446.5	0.0103	TESS	2459801.2989	9473	0.0098	TESS
2459772.6605	9410.5	0.0104	TESS	2459789.3850	9447	0.0097	TESS	2459801.5282	9473.5	0.0100	TESS
2459772.8895	9411	0.0103	TESS	2459789.6144	9447.5	0.0101	TESS	2459801.5282	9473.5	0.0100	TESS
2459773.1182	9411.5	0.0100	TESS	2459789.8432	9448	0.0097	TESS	2459801.7576	9474	0.0103	TESS
2459773.3471	9412	0.0097	TESS	2459790.0727	9448.5	0.0101	TESS	2459801.7576	9474	0.0103	TESS
Min.	Epoch	$O-C$	Reference	Min.	Epoch	$O-C$	Reference	Min.	Epoch	$O-C$	Reference
2459801.9868	9474.5	0.0103	TESS	2459809.0894	9490	0.0104	TESS	2459817.3373	9508	0.0103	TESS
2459801.9868	9474.5	0.0103	TESS	2459809.3179	9490.5	0.0098	TESS	2459817.3373	9508	0.0103	TESS
2459802.2160	9475	0.0104	TESS	2459809.3179	9490.5	0.0098	TESS	2459817.5658	9508.5	0.0096	TESS
2459802.2162	9475	0.0106	TESS	2459809.5474	9491	0.0102	TESS	2459817.5660	9508.5	0.0098	TESS
2459802.4448	9475.5	0.0101	TESS	2459809.5474	9491	0.0102	TESS	2459817.7953	9509	0.0100	TESS
2459802.4453	9475.5	0.0106	TESS	2459809.7764	9491.5	0.0101	TESS	2459817.7953	9509	0.0100	TESS
2459802.6743	9476	0.0104	TESS	2459809.7764	9491.5	0.0101	TESS	2459818.0240	9509.5	0.0096	TESS
2459802.6744	9476	0.0105	TESS	2459810.9223	9494	0.0104	TESS	2459818.0241	9509.5	0.0097	TESS
2459802.9033	9476.5	0.0104	TESS	2459810.9225	9494	0.0106	TESS	2459818.2532	9510	0.0097	TESS
2459802.9033	9476.5	0.0104	TESS	2459811.1506	9494.5	0.0096	TESS	2459818.2532	9510	0.0097	TESS
2459803.1325	9477	0.0104	TESS	2459811.1506	9494.5	0.0096	TESS	2459818.4825	9510.5	0.0099	TESS
2459803.1326	9477	0.0106	TESS	2459811.3801	9495	0.0100	TESS	2459818.4825	9510.5	0.0099	TESS
2459803.3609	9477.5	0.0097	TESS	2459811.3801	9495	0.0100	TESS	2459818.7120	9511	0.0103	TESS
2459803.3610	9477.5	0.0098	TESS	2459811.6093	9495.5	0.0100	TESS	2459818.7120	9511	0.0103	TESS
2459803.5900	9478	0.0097	TESS	2459811.6093	9495.5	0.0100	TESS	2459818.9413	9511.5	0.0105	TESS
2459803.5900	9478	0.0097	TESS	2459811.8387	9496	0.0103	TESS	2459818.9413	9511.5	0.0105	TESS
2459803.8195	9478.5	0.0101	TESS	2459811.8387	9496	0.0103	TESS	2459819.1702	9512	0.0102	TESS
2459803.8195	9478.5	0.0101	TESS	2459812.0679	9496.5	0.0104	TESS	2459819.1702	9512	0.0102	TESS
2459804.0484	9479	0.0099	TESS	2459812.0679	9496.5	0.0104	TESS	2459819.3994	9512.5	0.0103	TESS
2459804.0484	9479	0.0099	TESS	2459812.2962	9497	0.0096	TESS	2459819.3996	9512.5	0.0105	TESS
2459804.2776	9479.5	0.0099	TESS	2459812.2963	9497	0.0097	TESS	2459819.6284	9513	0.0102	TESS
2459804.2776	9479.5	0.0099	TESS	2459812.5254	9497.5	0.0097	TESS	2459819.6284	9513	0.0102	TESS
2459804.5071	9480	0.0104	TESS	2459812.5254	9497.5	0.0097	TESS	2459819.8574	9513.5	0.0101	TESS
2459804.5073	9480	0.0106	TESS	2459812.7542	9498	0.0094	TESS	2459819.8578	9513.5	0.0105	TESS
2459804.7361	9480.5	0.0103	TESS	2459812.7547	9498	0.0099	TESS	2459820.0865	9514	0.0101	TESS
2459804.7361	9480.5	0.0103	TESS	2459812.9835	9498.5	0.0096	TESS	2459820.0865	9514	0.0101	TESS
2459804.9650	9481	0.0100	TESS	2459812.9836	9498.5	0.0097	TESS	2459820.3161	9514.5	0.0105	TESS
2459804.9650	9481	0.0100	TESS	2459813.2135	9499	0.0105	TESS	2459820.3162	9514.5	0.0106	TESS
2459805.1945	9481.5	0.0104	TESS	2459813.2136	9499	0.0106	TESS	2459820.5443	9515	0.0096	TESS
2459805.1945	9481.5	0.0104	TESS	2459813.4419	9499.5	0.0098	TESS	2459820.5443	9515	0.0096	TESS
2459805.4233	9482	0.0101	TESS	2459813.4419	9499.5	0.0098	TESS	2459820.7741	9515.5	0.0103	TESS
2459805.4233	9482	0.0101	TESS	2459813.6715	9500	0.0102	TESS	2459820.7741	9515.5	0.0103	TESS
2459805.6528	9482.5	0.0105	TESS	2459813.6715	9500	0.0102	TESS	2459821.0030	9516	0.0101	TESS

Table 7
(Continued)

Min.	Epoch	$O-C$	Reference	Min.	Epoch	$O-C$	Reference	Min.	Epoch	$O-C$	Reference
2459805.6529	9482.5	0.0106	TESS	2459813.9000	9500.5	0.0097	TESS	2459821.0030	9516	0.0101	TESS
2459805.8812	9483	0.0098	TESS	2459813.9000	9500.5	0.0097	TESS	2459821.2322	9516.5	0.0102	TESS
2459805.8812	9483	0.0098	TESS	2459814.1296	9501	0.0102	TESS	2459821.2326	9516.5	0.0106	TESS
2459806.1110	9483.5	0.0105	TESS	2459814.1296	9501	0.0102	TESS	2459821.4612	9517	0.0101	TESS
2459806.1111	9483.5	0.0106	TESS	2459814.3589	9501.5	0.0103	TESS	2459821.4612	9517	0.0101	TESS
2459806.3398	9484	0.0101	TESS	2459814.3589	9501.5	0.0103	TESS	2459821.6902	9517.5	0.0099	TESS
2459806.3398	9484	0.0101	TESS	2459814.5881	9502	0.0104	TESS	2459821.6902	9517.5	0.0099	TESS
2459806.5684	9484.5	0.0096	TESS	2459814.5882	9502	0.0105	TESS	2459821.9197	9518	0.0104	TESS
2459806.5686	9484.5	0.0098	TESS	2459814.8165	9502.5	0.0097	TESS	2459821.9199	9518	0.0106	TESS
2459806.7976	9485	0.0097	TESS	2459814.8165	9502.5	0.0097	TESS	2459822.1482	9518.5	0.0098	TESS
2459806.7976	9485	0.0097	TESS	2459815.0456	9503	0.0097	TESS	2459822.1482	9518.5	0.0098	TESS
2459807.0269	9485.5	0.0099	TESS	2459815.0456	9503	0.0097	TESS	2459822.3780	9519	0.0104	TESS
2459807.0269	9485.5	0.0099	TESS	2459815.2752	9503.5	0.0102	TESS	2459822.3781	9519	0.0106	TESS
2459807.2562	9486	0.0101	TESS	2459815.2752	9503.5	0.0102	TESS	2459822.6071	9519.5	0.0104	TESS
2459807.2562	9486	0.0101	TESS	2459815.5041	9504	0.0099	TESS	2459822.6071	9519.5	0.0104	TESS
2459807.4849	9486.5	0.0097	TESS	2459815.5041	9504	0.0099	TESS	2459822.8358	9520	0.0100	TESS
2459807.4850	9486.5	0.0098	TESS	2459815.7337	9504.5	0.0104	TESS	2459822.8358	9520	0.0100	TESS
2459807.7147	9487	0.0104	TESS	2459815.7338	9504.5	0.0105	TESS	2459823.0653	9520.5	0.0104	TESS
2459807.7148	9487	0.0105	TESS	2459815.9627	9505	0.0103	TESS	2459823.0654	9520.5	0.0105	TESS
2459807.9438	9487.5	0.0104	TESS	2459815.9627	9505	0.0103	TESS	2459823.2943	9521	0.0103	TESS
2459807.9440	9487.5	0.0106	TESS	2459816.1919	9505.5	0.0104	TESS	2459823.2943	9521	0.0103	TESS
2459808.1726	9488	0.0101	TESS	2459816.1921	9505.5	0.0106	TESS	2459823.5231	9521.5	0.0100	TESS
2459808.1726	9488	0.0101	TESS	2459816.4210	9506	0.0104	TESS	2459823.5231	9521.5	0.0100	TESS
2459808.4015	9488.5	0.0098	TESS	2459816.4210	9506	0.0104	TESS	2459823.7522	9522	0.0100	TESS
2459808.4015	9488.5	0.0098	TESS	2459816.6501	9506.5	0.0104	TESS	2459823.7522	9522	0.0100	TESS
2459808.6304	9489	0.0096	TESS	2459816.6501	9506.5	0.0104	TESS	2459823.9818	9522.5	0.0104	TESS
2459808.6305	9489	0.0097	TESS	2459816.8792	9507	0.0104	TESS	2459823.9818	9522.5	0.0104	TESS
2459808.8601	9489.5	0.0102	TESS	2459816.8794	9507	0.0106	TESS	2459824.2103	9523	0.0098	TESS
2459808.8601	9489.5	0.0102	TESS	2459817.1083	9507.5	0.0104	TESS	2459824.2103	9523	0.0098	TESS
2459809.0894	9490	0.0104	TESS	2459817.1083	9507.5	0.0104	TESS				

ORCID iDs

Atila Poro https://orcid.org/0000-0002-0196-9732
Mehmet Tanriver https://orcid.org/0000-0002-3263-9680
Elham Sarvari https://orcid.org/0009-0006-1033-5885
Shayan Zavvarei https://orcid.org/0009-0002-2937-9053
Hossein Azarara https://orcid.org/0009-0003-2631-6329
Laurent Corp https://orcid.org/0009-0003-8727-410X
Sabrina Baudart https://orcid.org/0009-0004-8426-4114
Asma Ababafi https://orcid.org/0009-0004-8579-7692
Nazanin Kahali Poor https://orcid.org/0009-0007-5785-7303
Fariba Zare https://orcid.org/0009-0005-4980-0273
Ahmet Bulut https://orcid.org/0000-0002-7215-926X
Ahmet Keskin https://orcid.org/0000-0002-9314-0648

References

Akerlof, C., Amrose, S., Balsano, R., et al. 2000, AJ, 119, 1901
Albayrak, B., Yuce, K., Selam, S. O., et al. 2005, IBVS, 5649, 1
Applegate, J. H. 1992, ApJ, 385, 621
Arena, C., Aceti, P., Banfi, M., et al. 2011, IBVS, 5997, 1
Banfi, M., Aceti, P., Arena, C., et al. 2012, IBVS, 6033, 1
Biro, I. B., Borkovits, T., Csizmadia, S., et al. 2006, IBVS, 5684, 1
Biro, I. B., Borkovits, T., Hegedus, T., et al. 2007, IBVS, 5753, 1
Bond, H. 1976, IBVS, 1214, 1
Borkovits, T., Biro, I. B., Csizmadia, S., et al. 2004, IBVS, 5579, 1
Borkovits, T., Biro, I. B., Hegedus, T., et al. 2002, IBVS, 5313, 1
Castelli, F., & Kurucz, R. L. 2004, A&A, 419, 725
Cifuentes, C., Caballero, J. A., Cortés-Contreras, M., et al. 2020, A&A, 642, A115
Conroy, K. E., Kochoska, A., Hey, D., et al. 2020, ApJS, 250, 34
Cox, A. N. 2020, Allen's Astrophysical Quantities (AN Cox ed) (Berlin: Springer)
Deb, S., & Singh, H. P. 2011, MNRAS, 412, 1787
Demircan, O., Selam, S., & Derman, E. 1991, Ap&SS, 186, 57
Demircan, O., Tanriver, M., Devlen, A., et al. 1994, IBVS, 4126, 1
Derman, E., Demircan, O., & Selam, S. 1991, A&As, 90, 301
Devor, J., Charbonneau, D., O'Donovan, F. T., Mandushev, G., & Torres, G. 2008, AJ, 135, 850
Diethelm, R. 2001, IBVS, 5027, 1
Drozdz, M., & Ogloza, W. 2005, IBVS, 5623, 1
Dryomova, G. N., & Svechnikov, M. A. 2006, Ap, 49, 358
Dvorak, S. W. 2003, IBVS, 5378, 1
Dvorak, S. W. 2004, IBVS, 5502, 1
Eker, Z., Bakış, V., Bilir, S., et al. 2018, MNRAS, 479, 5491
Eker, Z., Demircan, O., Bilir, S., & Karataş, Y. 2006, MNRAS, 373, 1483
Flower, P. J. 1996, ApJ, 469, 355
Gazeas, K., & Stępień, K. 2008, MNRAS, 390, 1577
George, D. B. 2000, IAPPP, 79, 2
Gessner, H. 1966, VeSon, 7, 61
Green, G. M., Schlafly, E., Zucker, C., Speagle, J. S., & Finkbeiner, D. 2019, ApJ, 887, 93
Heckert, P. 1994, IBVS, 4127, 1
Hoffmeister, C. 1963, AN, 287, 169
Hubscher, J., Lehmann, P. B., Monninger, G., Steinbach, H.-M., & Walter, F. 2010, IBVS, 5941, 1
Kiss, L. L., Kaszas, G., Furesz, G., & Vinko, J. 1999, IBVS, 4681, 1
Kouzuma, S. 2018, PASJ, 70, 90
Kreiner, J. M., Kim, C.-H., & Na, I.-s. 2001, An Atlas of OC Diagrams of Eclipsing Binary Stars (Wydaw. Naukowe Akademii Pedagogicznej)
Latković, O., Čeki, A., & Lazarević, S. 2021, ApJS, 254, 10
Li, K., Xia, Q.-Q., Kim, C.-H., et al. 2021, AJ, 162, 13
Lu, W., & Rucinski, S. M. 1999, AJ, 118, 515
Lucy, L. B. 1967, ZAp, 65, 89
Lucy, L. B. 1968, ApJ, 151, 1123
Maceroni, C., & van't Veer, F. 1996, A&A, 311, 523
Maciejewski, G., & Karska, A. 2004, IBVS, 5494, 1
Mamajek, E. 2022, University of Rochester
Muyesseroglu, Z., & Selam, S. O. 1994, IBVS, 4027, 1
Nelson, R. H. 2015, IBVS, 6131, 1
O'Connell, D. J. K. 1951, PRCO, 2, 85
Ozavci, I., Bahar, E., Izci, D. D., et al. 2019, OEJV, 203, 1
Paczyński, B. 1971, ARA&A, 9, 183
Parimucha, S., Dubovsky, P., Baludansky, D., et al. 2009, IBVS, 5898, 1
Parimucha, S., Dubovsky, P., Vanko, M., et al. 2011, IBVS, 5980, 1
Parimucha, S., Dubovsky, P., & Vanko, M. 2013, IBVS, 6044, 1
Pecaut, M. J., & Mamajek, E. E. 2013, ApJS, 208, 9
Poro, A., Paki, E., Alizadehsabegh, A., et al. 2024b, RAA, 24, 015002
Poro, A., Tanriver, M., Michel, R., & Paki, E. 2024a, PASP, 136, 024201
Pribulla, T., Kreiner, J. M., & Tremko, J. 2003, CoSka, 33, 38
Prša, A., Conroy, K. E., Horvat, M., et al. 2016, ApJS, 227, 29
Qian, S. 2001, MNRAS, 328, 635
Qian, S. 2003, MNRAS, 342, 1260
Ruciński, S. M. 1969, AcA, 19, 245
Samolyk, G. 2016, JAAVSO, 44, 69
Samolyk, G. 2017, JAAVSO, 45, 121
Samolyk, G. 2020, JAAVSO, 48, 256
Selam, S. O., Gurol, B., & Muyesseroglu, Z. 1999, IBVS, 4670, 1
Sezer, C., Gulmen, O., & Gudur, N. 1984, IBVS, 2553, 1
Soomandar, S., & Poro, A. 2024, NewA, 105, 102112
Wang, R., Lu, W., & Fan, Q. 1987, IBVS, 2982, 1
Wieck, M., & Wunder, E. 1989, IBVS, 3406, 1
Wilson, R. E. 1990, ApJ, 356, 613
Yilmaz, M., Basturk, O., Alan, N., et al. 2009, IBVS, 5887, 1
Zhou, X., Qian, S. B., Zhang, J., et al. 2016, ApJ, 817, 133